2017-01-01

Flexible Analysis of Creep Rupture Database and Accelerating the Acquisition of Creep Rupture Data

Christopher Ramirez
University of Texas at El Paso, ramirez.christopher@gmail.com

FLEXIBLE ANALYSIS OF CREEP RUPTURE DATABASE AND

ACCELERATING THE ACQUISITION OF

CREEP RUPTURE DATA

CHRISTOPHER RAMIREZ

Master's Program in Mechanical Engineering

APPROVED:

Calvin M. Stewart, Ph.D., Chair

Jack Chessa, Ph.D.

Binata Joddar, Ph.D.

Charles H. Ambler, Ph.D.
Dean of the Graduate School

FLEXIBLE ANALYSIS OF CREEP RUPTURE DATABASE AND ACCELERATING THE ACQUISITION OF CREEP RUPTURE DATA

by

CHRISTOPHER RAMIREZ, BACHELOR OF SCIENCE IN PHYSICS

THESIS

Presented to the Faculty of the Graduate School of

The University of Texas at El Paso

in Partial Fulfillment

of the Requirements

for the Degree of

MASTER OF SCIENCE

Mechanical Engineering

THE UNIVERSITY OF TEXAS AT EL PASO

August 2017

Abstract

A comprehensive statistical analysis of creep data is a difficult task because there are many layers of uncertainty for a given dataset. Sources of uncertainty are inherent in both the databases that provide data, and the data themselves. Additionally, creep rupture predictions made with time-temperature parameter (TTP) models add an additional layer of uncertainty due to the fundamentally different ways in which each TTP model predicts creep behavior. A set of guidelines from the ECCC currently exist for such analyses, but they are best suited for narrowly-defined datasets. In this study, a broader set of guidelines are developed to analyze a large database of creep rupture data using the Larson-Miller Parameter. The guidelines are applied to a dataset of 316 stainless steel, which is collected across multiple public and private databases. The properties of the dataset are analyzed by comparing its statistical properties to that of the full dataset to subsets of form, thermomechanical processing, and chemistry metadata. The predictive ability of eight TTP models is analyzed by running nine combinations of isotherm and data culling conditions through each model. Recommendations are made in expanding the breadth of these guidelines. Acquiring the necessary creep rupture data to perform such a large analysis is time- and energy-expensive. Depending on the design specifications of a component, creep rupture can take anywhere between 10,000 to over 300,000 hours to occur. An accelerated creep test that accurately predicts the creep deformation and life of metallic materials is desired. This study also proposes modifying the Stepped Isostress Method designed for polymers to work for metallic materials in general. Experimental evidence is provided using 304SS subjected to 600°C. Monotonic tensile and conventional creep tests are conducted to establish baseline properties. Stepped Isostress Method tests are conducted and analytically adjusted to produce accelerated creep deformation and rupture data. Recommendations concerning future work on SSM are provided.

Keywords: 304SS, 316SS; creep rupture; master models; metadata; accelerated testing

Table of Contents

Chapter 1: Flexible Analysis of Creep Database

Introduction

Conventional approaches to design against creep deformation and rupture involve the long-term creep testing of multiple specimens. Depending on the expected service conditions and service life of a component, a single creep test can take up to and beyond 100,000 hours. To truly characterize the creep resistance of a material, many combinations of stress and temperature must be tested so that constitutive and life prediction models can be calibrated.

Accelerated Creep Testing (ACT) is a well-established method to estimate the creep strain and rupture properties of alloys used in the power generation industry [1]. The ACT tests are conventional creep tests conducted at a higher temperature and/or stress, the results of which are extrapolated to low temperature and/or stress conditions. International standards such as the ASME B&PV III, French RCC-MR, and British R5 recommend a phenomenological approach to creep where short-term creep data is extrapolated to long-term using predictive models, regression analysis, and confidence bands to manage reliability and preserve conservatism [2-5]

The ability of ACT to provide accurate predictions is limited by several factors. The predictions made by ACT assume the deformation mechanism which drives creep remains constant. Most ACT models are phenomenological and do not consider material properties nor the inherent randomness of the parameters. Probabilistic models have been developed to determine reliability, which incorporate the dispersion of the parameters and the scatter of the data with respect to an ACT master curve. However, these probabilistic models generally consider a limited number of ACT models for creep rupture extrapolation [6-10]. It is valuable to identify and examine how each source of uncertainty affects the predictive abilities of ACT models.

Sources of uncertainty inherent to the material (such as the material form, chemical composition, thermomechanical processing, etc.) can have a measurable impact on creep rupture behavior. For instance, alloying 316SS with nitrogen (i.e. 316N) demonstrates improved rupture life, lower minimum creep strain rate, reduced ductility, and decreased internal and surface creep damage [11-14]. The heat treatment of steels, especially alloys, enables the microstructure to be manipulated by controlling the rate of diffusion and cooling. Plastically working metals enables more robust microstructures to be developed, typically by closing cavities, elongating inclusions to parallel strings, and reducing grain size [15]. Typically, creep rupture predictions made with ACT models consider only the type of data that is used for the given application.

The uncertainty of the ACT parameters and inherent material properties means creep rupture data from many sources to accurately describe the creep response of a material. Ideally, creep rupture test data subject to identical testing conditions should not vary from organizations to organization, especially because the only two experimental variables are stress and temperature. However, there are clear variations when analyzing the data between organizations [16]. Organizations such as the European Creep Collaborative Committee (ECCC) has taken steps to standardize the acquisition, organization, and analysis of creep data from multiple organizations—in part—to accurately determine the long-term creep rupture properties of alloys used in the power generation industry [17]. Collaborative efforts such as this are vital to the development of more realistic ACT prediction models, especially because creep rupture data is expensive and time-consuming to produce in-house.

In this study, the accuracy of a creep rupture dataset for alloy 316SS, acquired from multiple sources, is analyzed using eight time-temperature parameter models. The ability of each model to interpolate and extrapolate creep rupture is examined by running nine combinations of

isotherm and data culling conditions through each model. The statistical properties of the dataset are analyzed using the guidelines from the ECCC. Several subsets of the dataset are considered with respect to form, thermomechanical processing, and chemistry.

Creep Data

Data Sources

To perform a thorough assessment of creep rupture data, creep rupture data was collected from databases, material handbooks, and technical documents. A list of these sources, and the number of data points collected from each are listed in Table 1.

Table 1- Data by source [18 - 23]

Source	ASM Atlas of Creep	ASTM DS5-S1	ASTM STP 552	ASTM STP 124	NIMS	ORNL-5237
No. Data Points	41	547	215	236	1208	41

Established databases are the highest priority because they contain large amounts of reliable data that have been vetted. Reliable data is defined as information presented as unambiguous numerical values, as opposed to data presented graphically (e.g. plots). In most instances, data from established databases are tabulated and source files are digitized, which facilitates accurate and efficient data acquisition. Conversely, sources such as journal articles and dissertations seldom provide tabulated data and typically present information as plots. To acquire this data and implement it into TTP models, open-source data extraction software should be used to convert the plots into tabulated data [24]. These data sources are deemed “unreliable” because of the subjectivity involved in manually selecting data points, defining the start and end points on a curve, and defining the reference axes. Data extraction software thus introduces uncertainty and lowers the accuracy of data. Data that is collected in this manner should be marked accordingly in the data assessment because they may prove to be outliers.

Metadata

The variability in creep rupture is often defined as the spread of a dataset. Variability depends on material properties, experimental parameters, and non-experimental parameters, which are collectively referred as "metadata". Acquiring metadata is crucial because it can help identify sources of uncertainty for a given material. Additionally, calibration of TTP models—and thus their predictive ability—are affected by choice of input rupture data, the properties of which are determined by metadata. The metadata identified in this study, along with a brief description and the expected impact on its test results, are listed in Table 2.

Table 2- Summary of metadata under consideration

Metadata Category	Description
Alloy name	Unabbreviated name of a material
Material code	Material trade name
Country code	Location where stock material was made
Laboratory code	Location where test took place
Material Spec/Grade	Classification of a material by its composition and physical properties
Chemical composition	Detailed chemical stoichiometry of a material
Thermomechanical processing	Metallurgical process that influences the microstructure of a material by applying mechanical deformation and/or heat treatments
Form	Shape of test specimen
Test type	Classification of the mechanical deformation (creep, creep-fatigue, fatigue)
Test standard	Standardized guidelines to performing laboratory tests and interpreting the results
Specimen geometry	Size of specimen
Test equipment	Specifications of the machine on which the test took place (e.g. load cell resolution)
Environment	The physical surroundings in which the test takes place (e.g. cryogenic temperature, argon environment)

Each metadata category may contain subsets of metadata. For instance, form metadata includes specimens shaped as tubes, bar, etc. To understand the impact of metadata on creep rupture variability, each category should be examined independently to determine what—if any—patterns exist. The effects of metadata on creep rupture can be generalized to how a specific

metadata affects the mechanical properties of the material, which will ultimately affect its plastic response. Two primary sources that affect the material properties of anisotropy and chemistry. Crystallographic anisotropy (i.e. texturing) manifests as the random orientation of grains which can be deformed during processing. Mechanical anisotropy is produced by the deformation of inclusions or second-phase particles along specific directions [25]. Both texturing and mechanical anisotropy are influenced by deformation processes; it follows that metadata representative of changes in anisotropy should have a measurable impact on test results. Chemistry affects a material's fundamental resistance to oxygen diffusion, which affect deformation processes and aging for long-term creep. Thus, this study will analyze three metadata categories that follow this reasoning: form, thermomechanical processing, and chemistry. From each of these metadata, a subset is chosen based on the highest number of data points, which are tube form, hot-rolled thermomechanical processing, and nitrogen-alloyed chemistry.

Creep Models

The extrapolation of ACT data to predict low stress and temperature rupture is performed using predictive models. Master curve models are the most commonly employed, where the relationships between stress, temperature, rupture time, minimum creep strain rate, and/or creep deformation are parameterized onto a single curve. Time-temperature parameter (TTP) models are a form of master curve models where the isotherms of creep can be collapsed onto a single curve expressed as a function of stress. This function of stress is the stress parameter function, which enables the TTP models to make rupture time predictions at any stress and temperature condition. Master curve models are favored for their ability to predict long-term creep rupture using short-term creep rupture data, especially because creep mechanisms become more intense as temperature increases [26]. However, to calibrate the extrapolation, a sufficient number of midrange stress and

temperature creep tests must be performed to ensure the extrapolated creep rupture predictions are representative of actual material behavior. In addition, most models are phenomenological and do not consider creep mechanisms such as simulating the service failure mode, remaining in a single deformation mechanism zone, producing a realistic oxidation state, and replicating the metallurgical instabilities that develop at the target boundary conditions.

There are two main sources of uncertainty within TTPs: the relationships between the TTP variables and choice of stress parameterization function. Each model differently describes the relationships between temperature, stress, and creep rupture time, and the stress parameter function can take many forms (e.g. linear, polynomial, power, logarithmic and exponential functions) and can dramatically affect the predictive abilities of the TTP models [30]. Thus, creep rupture predictions will vary from model to model.

In this study, the predictive capabilities (i.e. integrity) of eight TTP models will be studied by examining their ability to provide consistent and accurate creep rupture predictions as the dataset is subject to several combinations of culling conditions. The models under consideration are listed in Table 3. A high integrity model should provide consistent creep rupture predictions despite changes in the dataset, while low integrity models should not under the same circumstances.

Table 3 – List of time-temperature parameter models [31-36]

Model	Parameter Equation
Larson-Miller (LM)	$P_{LMP} = T(\log(t_r) + t_a)$
Manson-Haferd (MH)	$P_{MH} = \frac{\log(t_r) - \log(t_a)}{T - T_a}$
Manson-Brown (MB)	$P_{MB} = \frac{\log(t_r) - \log(t_a)}{(T - T_a)^n}$
Orr-Sherby-Dorn (OSD)	$P_{OSD} = \log(t_r) - Q/RT$
Manson-Succop (MS)	$P_{MS} = \log(t_r) - BT$

Goldhoff-Sherby (GS)	$P_{GS} = \frac{\log(t_r) - \log(t_a)}{1/T - 1/T_a}$
Modified Manson-Haferd (MMH)	$P_{MMH} = \frac{\log(t_r) - \log(t_a)}{T}$
Modified Graham-Wallace (MGW)	$P_{MGW} = \frac{\log(t_r)}{(1/T - 1/T_a)^n}$

Guide to the Assessment of Data and Models

Effect of Metadata on Modeling

The effects of metadata on modeling be assessed using well-known descriptive statistics and recommendations made by the European Creep Collaborative Committee (ECCC) [17]. Per ECCC, the dataset is analyzed by constructing plots of predicted creep rupture versus observed rupture on a log-log scale. A linear regression is then constructed to obtain a mean line. It is recommended the model equation used to predict creep rupture should be reassessed if:

1. The slope of the mean line is less than 0.78 or greater than 1.22
2. More than 1.5% of the data points fall outside 2.5 standard deviations from the mean line (i.e. outliers)
3. The mean line is not contained within the log(2) boundary lines between $t_r = 100hr$ and $t_r = 100{,}000hr$

Creep rupture predictions are performed from 10 MPa to 1000 MPa of applied stress for the isotherms present in the full dataset, after isotherm merging. In this study, the Larson-Miller parameter (LMP) model is applied as follows

$$P_{LMP}(t_r) = T(\log(t_r) + t_a) \tag{1}$$

where P_{LMP} is the Larson-Miller parameter, T is absolute temperature, t_r is time to creep rupture, and t_a is a material constant; typically of the order 20 for metals. For all models, it is recommended

the material constants be determined analytically by fitting the creep rupture data to the parameter (P_{LMP} in this case) by using a least-squared error method.

The value of P_{LMP} is calculated for every creep rupture data point (T, t_r). A stress parameter function $P_{LMP} = f(\sigma)$ is fit to the calculated values of P_{LMP}. The stress parameter function fits a curve through the TTP model and can take one of many forms. A series of common stress parameter functions is listed in Table 4.

Table 4 – Stress parameter function types

Function Type	Equation
Linear	$a_0 + a_1\sigma$
Logarithm	$a_0 + a_1\sigma + a_2 \log(\sigma)$
Ploy-nominal	$a_0 + a_1\sigma + a_2\sigma^2$
Power	$a_0 + a_1\sigma^{a_2}$
Exponential	$a_0 + a_1 e^{a_2\sigma}$

To isolate the performance of the models, the form of the stress parameter function must remain constant for each model. Each culling condition will have a unique set of coefficients, but the form of the stress parameter function must not change. In this study, a logarithmic function is selected for the LMP model because it does not exhibit an inflection point [30]. The logarithmic stress parameter function takes the form

$$P_{LMP}(\sigma) = a_0 + a_1\sigma + a_2 \log(\sigma) \tag{2}$$

where a_0, a_1 , a_2 are the coefficients of the function, σ is stress, and log is the common logarithm. To predict rupture life, replace $P_{LMP}(t_r)$ in [Eq. (2)] with $P_{LMP}(\sigma)$ in [Eq. (3)], then rearrange to solve for rupture life. The predictive equation for creep rupture life follows:

$$t_r = 10^{P_{LMP}(\sigma)/T - t_a} \tag{3}$$

Using the process outlined above, allows rupture life to be predicted for any stress and temperature condition for all TTP models.

The integrity of the TTP models will be determined by their ability to provide consistent and accurate creep rupture predictions as the dataset used for extrapolation is changed. The normalized mean square error (NMSE) is used to quantify the accuracy of the models by comparing the creep rupture values predicted with a TTP model and the actual rupture time observed in the dataset. The NMSE is calculated by:

$$NMSE = \frac{\overline{(X-Y)^2}}{\overline{X}\cdot\overline{Y}} \tag{4}$$

where X is the experimental data, Y is the predicted data, and bars above a value represent taking the average. A value of zero for the NMSE indicates an exact prediction, while large values indicate a bad fit. Although there is no threshold where good NMSE values become bad, it has been suggested that the NMSE values be compared to the ratio of the observed versus the predicted.

Assessment of Models

Step 1: Import Raw Creep Rupture Dataset

The raw dataset should comply with three preliminary culls to facilitate creep rupture predictions. These are:

1. Checking that essential creep-rupture information is present - The essential information required to make creep rupture predictions are temperature, creep rupture time, and stress. Data points that do not contain this information must be disregarded. Tests marked as ongoing or discontinued are also disregarded because these data points will underestimate creep rupture predictions when using least-squares regression methods [37].
2. Culling by metadata (optional) - The resulting dataset (regardless if metadata is considered) is referred as the “full dataset”. From here, the dataset may be culled to consider a particular metadata. Metadata should be chosen such that the categories with a large number of

outliers should be reassessed. Outliers are defined as the data points that, when plotted as a linear regression of observed vs. predicted rupture time using a TTP model, fall outside 2.5 standard deviations from the mean line. Additionally, the number of data points per isotherm should be enough to ensure the least-squares method can be applied. The least-squares method requires that the number of data points must be greater than or equal to the number of material constants. The metamodel considers a maximum of 10 material constants, so for a dataset to be analyzed with all model, the number of data points for all isotherms must be at least 10. Isotherms not meeting this criterion are disregarded.

3. Merging isotherms - The isotherms of the dataset are then merged in accordance to ECCC guidelines, which states that temperatures within ±2°C of a primary temperature may be combined and considered a single isotherm [28]. The nominal temperature variation of most temperature control units is within this range. In this study, when merging isotherms, the primary temperature is identified as the isotherm with the most number of data points. For instance, if there are 8 data points for 565.5°C and 18 data points for 566°C, the datasets are combined and considered as 566°C with 26 data points.

Step 2: Cull by Isotherm

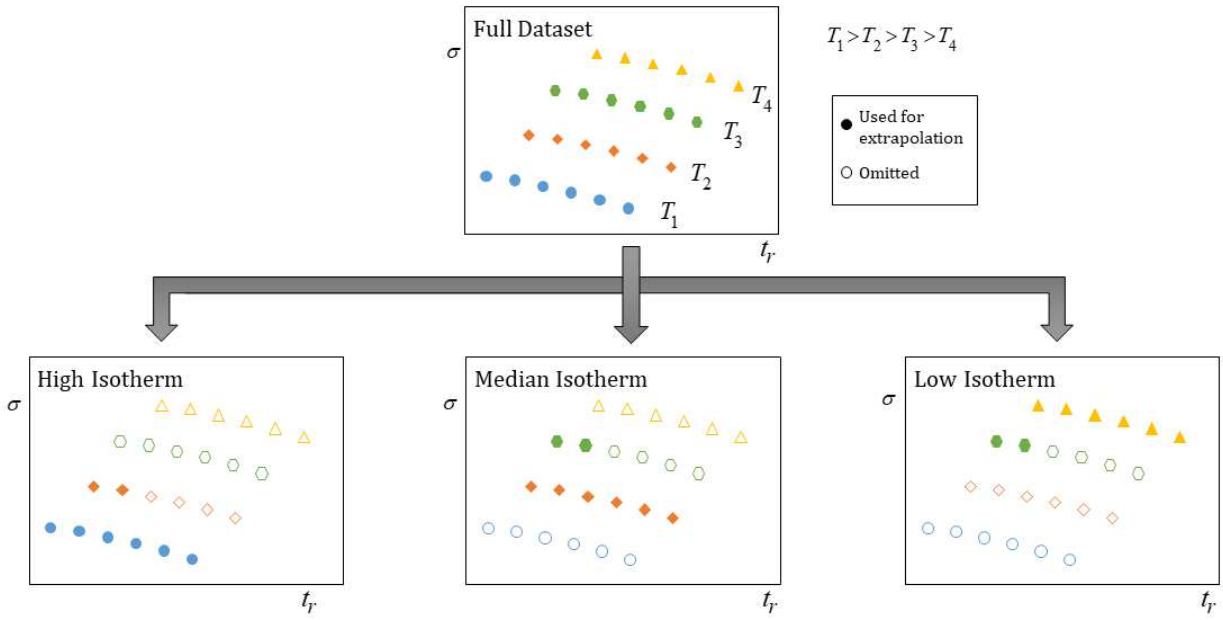

Figure 1 –Culling by isotherm

The temperature dependence of the models is analyzed by parsing the dataset to consider a limited number of isotherms. Some models do not perform well when considering one isotherm. The full dataset is culled to consider only two isotherms, a "main" and "supplementary" isotherm [38]. The supplementary isotherm is added because some models do not perform well using one isotherm. This culling process is shown in Figure 1. The main isotherm is defined as either the highest, median, or lowest isotherm of the full dataset, while the supplementary isotherm is dependent on the main isotherm. The supplementary isotherm is culled to consider only the shortest 1/3 of creep rupture data points. Culling by 1/3 ensures at least three data points remain per isotherm. Note that for datasets which do not have a median isotherm (that is, there are an even number of isotherms), the median is the higher temperature of the two middle isotherms.

Step 3: Simulate Limited Data Availability

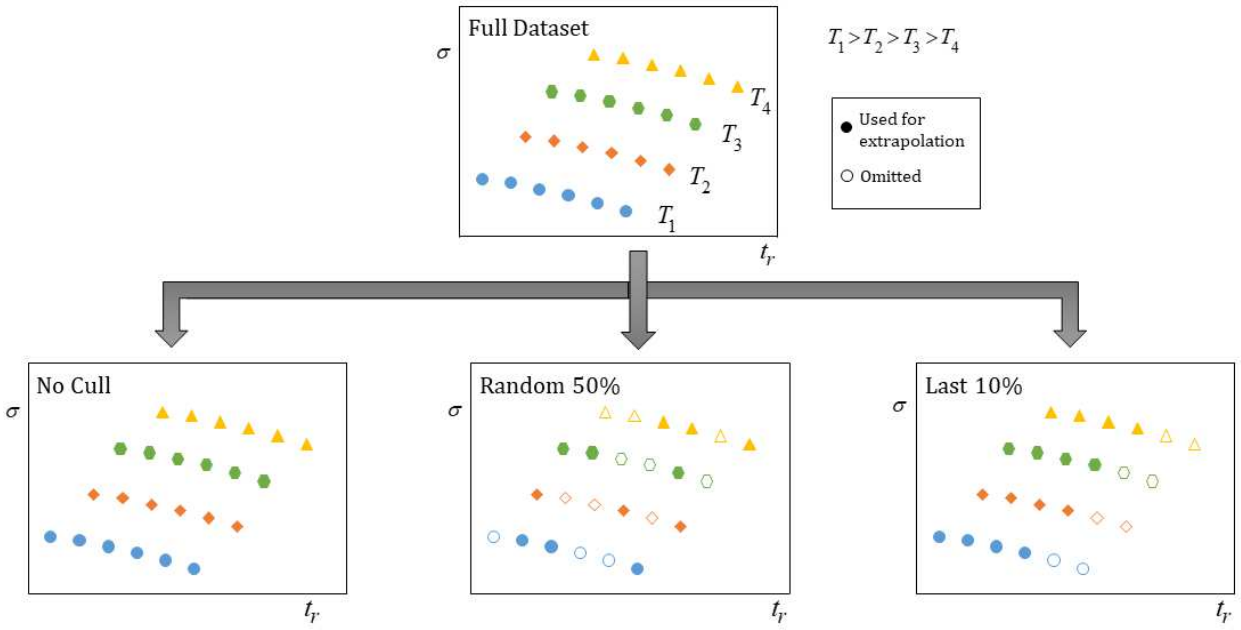

Figure 2 – Culling to simulate missing data

The integrity of the TTP models is further analyzed by simulating missing data points. The data culling procedure is illustrated in Figure 2. The resulting dataset is referred as the "culled dataset". Only data from the main isotherm is culled, under three separate conditions:

1. No cull – The main and supplementary isotherms are unmodified. The isotherm dataset contains the maximum number of data points and is thus the best-case scenario for creep rupture predictions.
2. Random 50% cull – From the main isotherm, a randomly selected 50% of data points are culled. The secondary isotherm is not culled. This evaluates the overall stability of the models when the number of data points is reduced.
3. Last 10% cull – From the main isotherm, 10% of the longest duration creep rupture data points are culled. That is, if creep rupture is sorted by increasing rupture time, the highest 10% of the data points are culled. The secondary isotherm is not culled. This cull evaluates whether creep rupture predictions become unstable as the most extreme data points are

removed. Recall that TTP models should not be used to extrapolate beyond the range of the dataset; it is important to see if a model can accurately recreate the material response at long life when the longest duration data points are removed.

Step 4: Creep Rupture Predictions using TTP Models, Full Dataset

Creep rupture predictions are made for (a) the full dataset and (b) each of the nine culled datasets. The procedure to make creep rupture predictions are detailed above, in the Effect of Metadata on Modeling section.

Step 5: Evaluate Physical Realism

Finally, the creep rupture predictions are checked to verify if the TTP models provided physically realistic results. The ECCC provides guidelines for physical realism, which recommends that:

1. Creep rupture predictions should be producible at temperatures $25°C$ above and below each isotherm
2. Isotherms should not cross over, come together, or turn back
3. The isotherms should not fall away too quickly unless the material is expected to exhibit sigmoidal behavior [28]

More recently, additional physical realism properties have been proposed where material properties are taken into consideration [40]. For instance, if the applied stress is equal to the tensile strength of the material, it follows that creep rupture should be approximately zero. A full list of these physical realism properties is provided in Table 5. Here, *UTS* is the ultimate tensile stress of the material, and T_m is its absolute melting temperature.

Table 5 – Physical realism conditions

Negative Stress	$\sigma < 0$	$t_r \approx \infty$
Zero Stress	$\sigma = 0$	$t_r = \infty$
Intermediate Stress	$0 < \sigma < UTS$	$t_r \propto f(\sigma, T)$
Ultimate Tensile Strength	$\sigma = UTS$	$t_r \approx 0$
Intermediate Temperature	$0.3T_m < T < T_m$	$t_r \propto f(\sigma, T)$
Absolute Melting Temperature	T_m	$t_r = 0$

Development of Algorithm

An algorithm is developed in Matlab to automatically perform the computational analyses. Using an algorithm provides multiple benefits: it reduces subjectivity by limiting human input; automates the process to save time; and easily expands to accommodate more experimental data, metadata, and constitutive models.

One unique aspect of the algorithm is the incorporation of a creep rupture "metamodel" developed by Shafinul Haque [39]. The metamodel unifies twelve creep rupture models into a single equation, the parameters of which can be changed to produce a desired TTP model equation. The equation for the metamodel is provided below:

$$P_{HS} = \frac{\log(t_r) - \alpha_0 - \alpha_1 T^r}{(T^r - {\alpha_2}^r)^q} \tag{5}$$

where P_{HS} is a general parameter, t_r is creep rupture time, T is test temperature, α_{0-2} are material constants, and r and q are integers taking the values of -1, 0, or 1, depending on which TTP model is desired. For instance, values of $q = 1$, $r = 1$ and $\alpha_1 = \alpha_2 = 0$ reproduce the Larson-Miller TTP:

$$P_{LMP} = T(\log(t_r) + t_a) \tag{6}$$

The metamodel constants for all eight models used in this study are provided in Table 6.

Table 6 – Metamodel constants

Larson-Miller (LM)	$\alpha_2 = \alpha_1 = 0 \; r = -1, q = 1$
Manson-Haferd (MH)	$\alpha_1 = 0 \; r = q = 1$
Manson-Brown (MB)	$\alpha_1 = 0, r = 1, \; q = n$
Orr-Sherby-Dorn (OSD)	$\alpha_0 = 0, r = -1, q = 0$
Manson-Succop (MS)	$\alpha_0 = \alpha_2 = 0, r = 1, q = 0$
Goldhoff-Sherby (GS)	$\alpha_1 = 0, r = -1, q = 1$
Modified Manson-Haferd (MMH)	$\alpha_2 = \alpha_1 = 0, r = 1, q = 1$
Modified Graham-Wallace (MGW)	$\alpha_0 = \alpha_1 = 0 \; r = -1, q = n$

One major benefit of incorporating the metamodel is its efficiency; only one TTP equation needs to be hard-coded into the algorithm while the parameters can be passed as variables. Additionally, the parameters need not strictly be integers and can be passed as a continuous variable of real numbers. In this way, it is possible to develop unique TTP models that are hybrids are the original eight.

Material

In this study, a dataset of 316SS ($N = 1300$) will be subject to the procedures outlined above. The typical chemical composition and material properties of 316SS are listed in Table 7 and Table 8, respectively. To investigate how choice of metadata affects the accuracy of creep rupture predictions, three metadata will be studied: bar form ($N = 490$), hot-rolled thermomechanical processing ($N = 482$), and 316N chemistry ($N = 74$). These metadata are chosen because they are expected to have a major contribution on creep rupture and they contain the most number of data points for their respective metadata category (form, thermomechanical processing, and chemistry).

Table 7 – Chemical composition of 316SS [41-44]

Element	C	Cr	Fe	Mn	Mo	Ni	P	S	Si
Wt. %	0.08	18 (max)	62	2	3 (max)	14 (max)	0.045	0.03	1

Table 8 – Material properties of 316SS [41-44]

UTS* (MPa)	Yield Strength* (MPa)	T_m (°C)
580	290	1370-1400

**Recorded at 25°C*

Results and Discussion

Effects of Metadata on Modeling

The full dataset is parsed into three subsets to determine the effects of metadata on modeling: tube form, hot-rolled TMP, and nitrogen-alloyed chemistry (316N). The LMP model and a logarithmic stress-parameter function are used to make creep rupture predictions. The LMP material constants, NMSE values per metadata subset, stress parameter plots, creep rupture predictions, and histogram distribution plots are shown in Table 9, Table 10, Figure 4, Figure 5, and Figure 6 respectively. Descriptive statistics for each metadata are listed in Table 11.

Table 9 – LMP material constants for metadata subsets

Dataset	t_a	a_0, a_1, a_2
Full	9.89	14330, -4.52, -2387
Tube Form	10.625	13763, -7.03, -1688
Hot-rolled TMP	11.262	17022, -2.36, -3413
316N	7.78	12458, -4.15, -2119

Table 10 – NMSE values for metadata subsets

Dataset	NMSE
Full	66.9
Tube Form	4.64
Hot-rolled TMP	99.3
316N	3.96

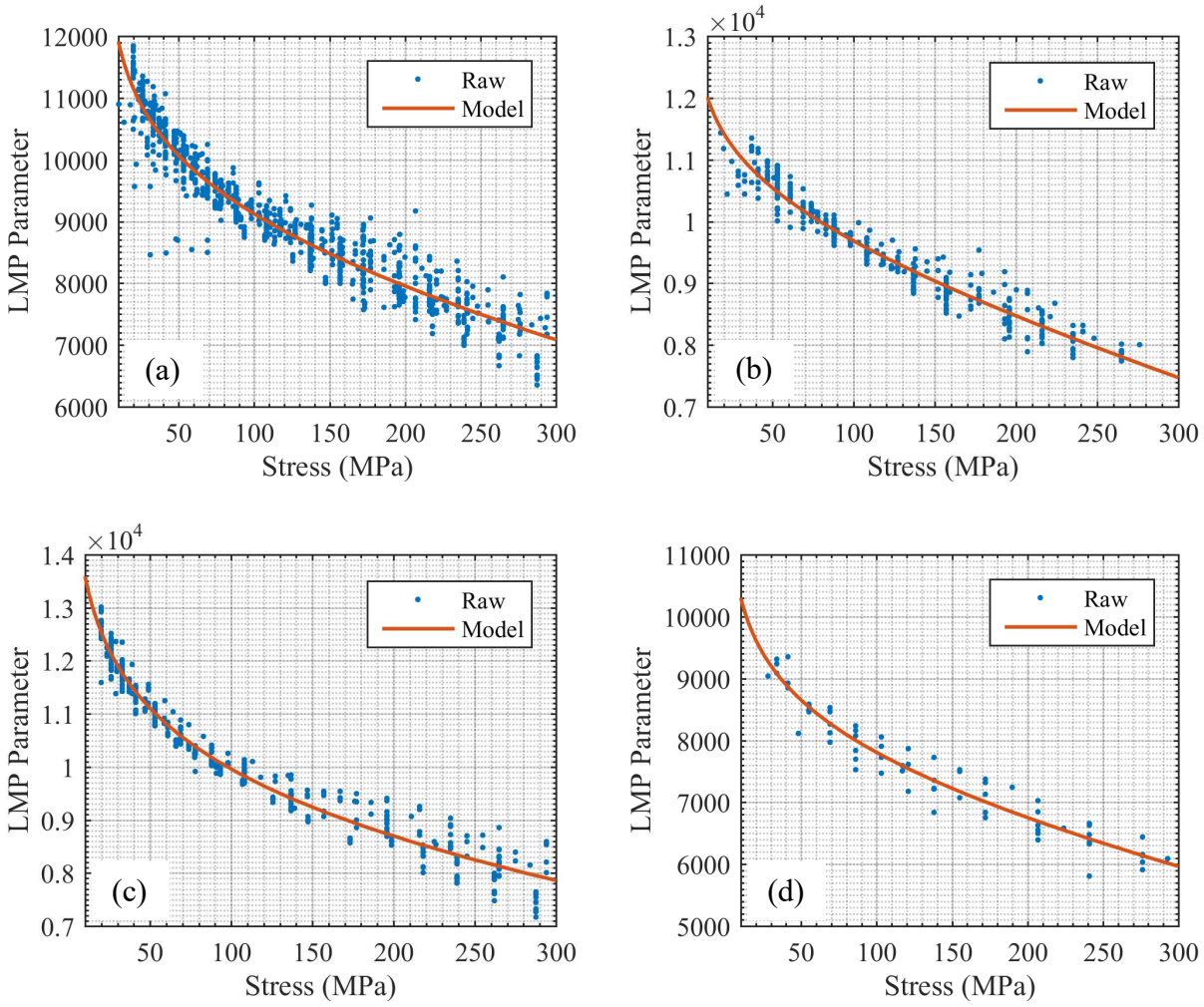

Figure 3 – Larson-Miller stress parameter of (a) full dataset (b) tube form (c) hot-rolled TMP (d) 316N chemistry

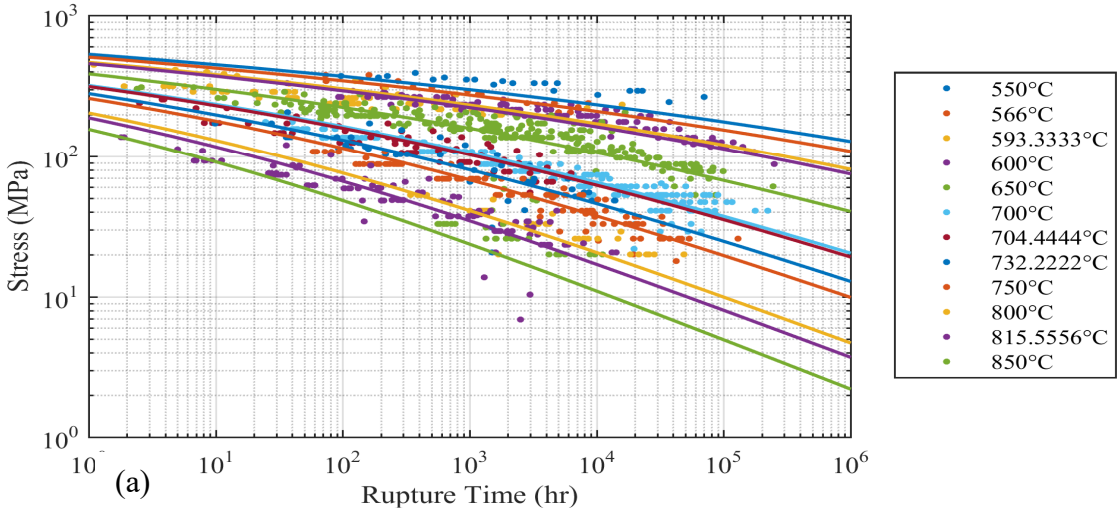

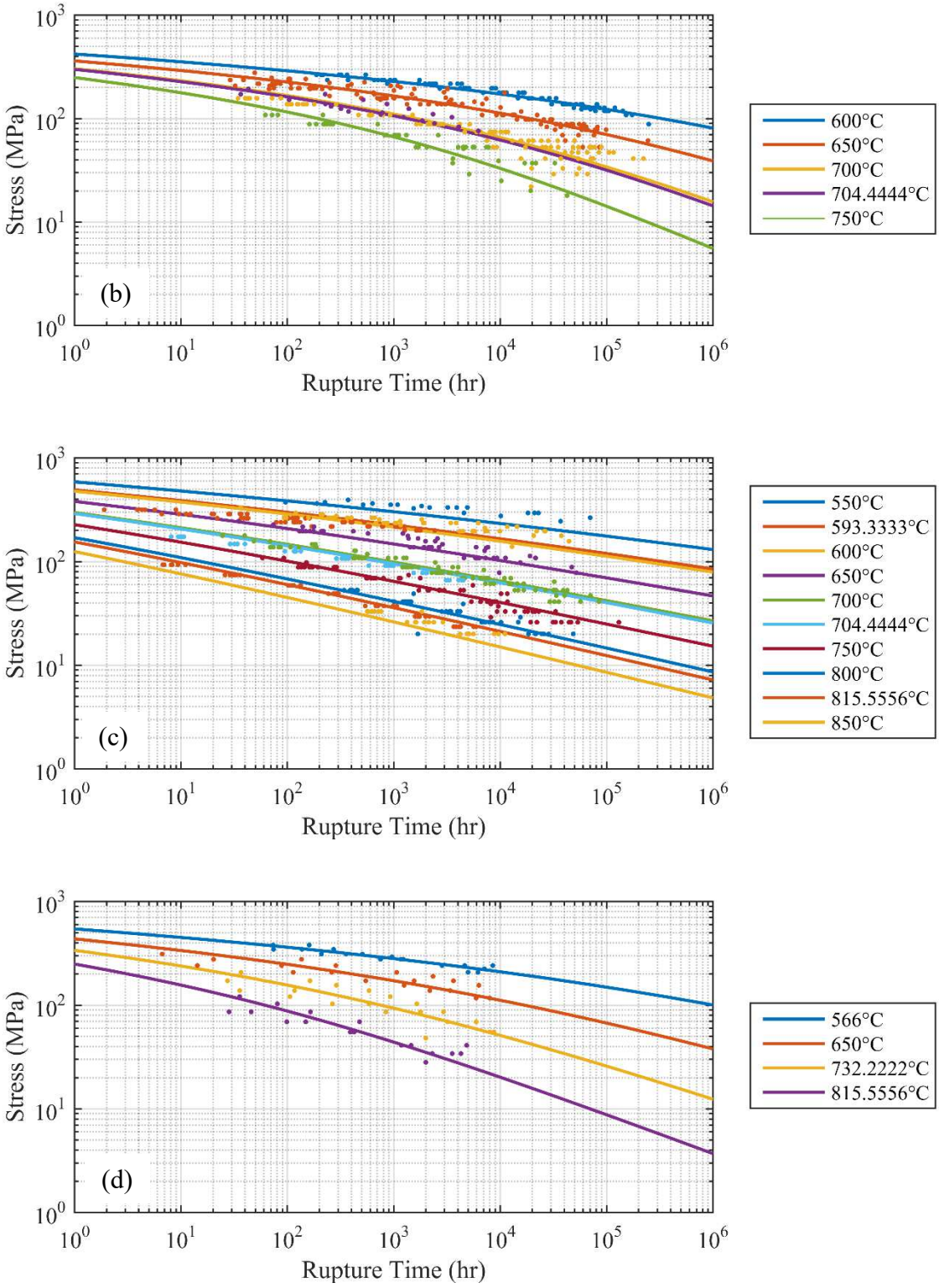

Figure 4 – Creep rupture predictions for (a) full dataset (b) tube form (c) hot-rolled TMP (d) 316N chemistry

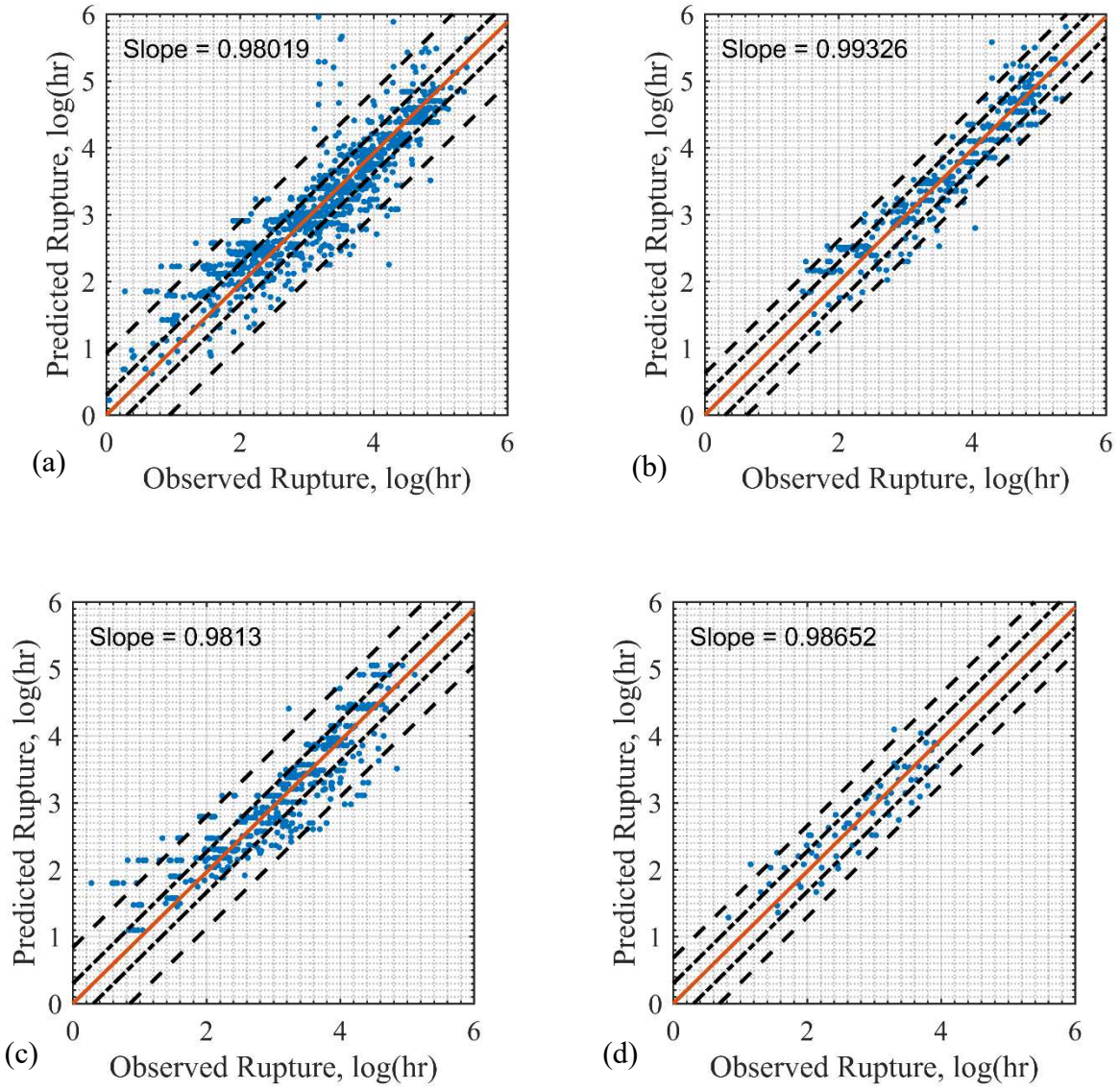

Figure 5 – Predicted vs. observed creep rupture for (a) full dataset (b) tube form (c) hot-rolled TMP (d) 316N chemistry

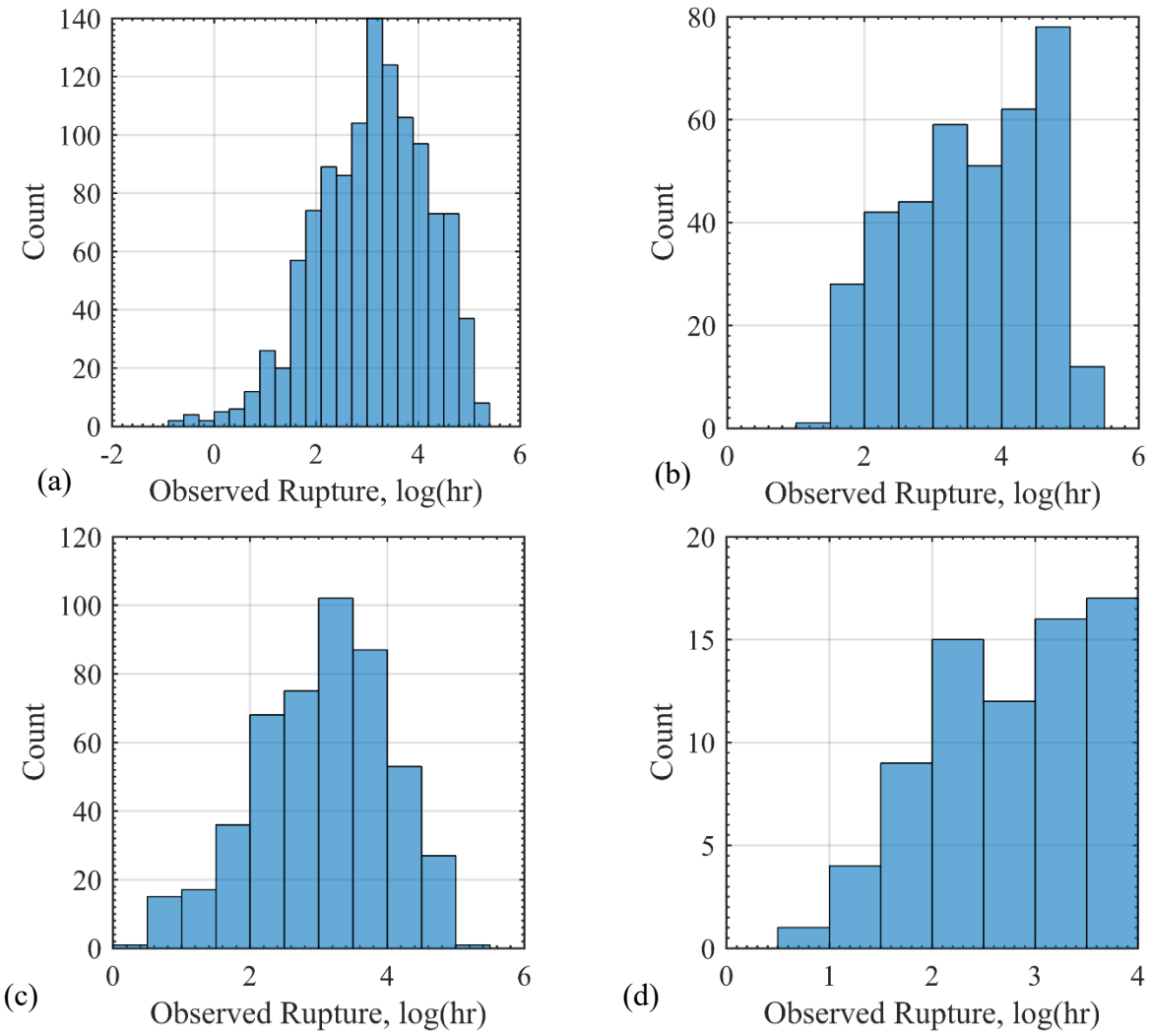

Figure 6 – Histogram distributions for (a) full dataset (b) tube form (c) hot-rolled TMP (d) 316N chemistry

Table 11 – Descriptive statistics of metadata subsets

Dataset	*N*	Mean, log(hr)	Std. Dev., log(hr)	Slope of Mean Line	Percent Outliers
Full	1145	3.102	1.079	0.98019	3.40
Tube Form	490	3.572	1.001	0.99326	1.06
Hot-rolled TMP	482	3.041	0.969	0.98130	4.77
316N	74	2.761	0.793	0.98652	2.70

First, the rupture predictions of the metadata subsets are discussed. A visual analysis is conducted as a preliminary assessment to gain an understanding of the significance of the

descriptive statistics. This will be followed by a more succinct analysis with respect to each metadata. As seen in Figure 4(a), creep rupture predictions for the full dataset appear physically realistic at first glance. No isotherms cross over, come together, or turn back. However, predictions for lowest and highest isotherms ($550\,°C$ and $850\,°C$) do not pass through some of their observed rupture times. The same behavior is observed for the hot-rolled TMP, but not for tube form or 316N chemistry. The predictive accuracy of each metadata can be determined quantitatively by their NMSE values. As seen in Table 10, NMSE values vary significantly for each metadata subset. The highest NMSE value (and thus the least accurate subset) is for the hot-rolled TMP dataset (NMSE = 99.3), while the lowest NMSE is for 316N chemistry (3.96). The full dataset has a relatively high NMSE value (NMSE = 66.9), and it is elucidating that the NMSE drops by an order of magnitude as the metadata is culled for either tube form or 316N. The implication of this observation is that selection of metadata can significantly affect the accuracy of a model.

Next, the linear regression of the observed rupture values vs. the predicted values is discussed. By observing the mean line of predicted rupture versus observed rupture (e.g. Table 5) one can determine whether the model effectively represents the behavior of a given dataset. It is observed that for all datasets the mean lines are very close to unity, and are contained within the $\pm\log(2)$ boundary lines between $t_r = 100\text{hr}$ and $t_r = 100{,}000\text{hr}$. Of the metadata subsets, tube form appears to conform the best to ECCC standards; the slope of the mean line is closest to unity (0.99326) and the percent outliers (1.06%) is the only one that is less than 1.5%. The other datasets show more variation in their properties. The hot-tolled TMP subset has the largest percent of outliers (4.77%) and the second-lowest standard deviation (0.969). The 316N subset has percent outliers (2.70%) that is almost three times that of tube form, despite having the smallest standard deviation (0.793).

Finally, the histogram distribution of the metadata subsets is discussed. The histogram distribution of the data (e.g. Figure 6) provides a visual representation of the scatter of the data. The histogram distribution of the full dataset and hot-rolled TMP dataset show a log-normal distribution centered around their respective means. However, the histogram distribution of tube form and 316N do not appear log-normally distributed. Both tube form and 316N metadata subsets are skewed, where more observed rupture times occur after the mean. For 316N, this behavior was expected because nitrogen is expected to improve the properties of 316SS. The implication of these skewed rupture times is that these metadata subsets may be more sensitive to data culling (i.e. culling for the longest 10% of the data).

Assessment of Models

The procedure for assessing the models is conducted in accordance with the steps outlined in Section 4.4. In assessing the integrity of the models, 10 sets of NMSE results are produced. One set of results stems from the full dataset, where all data points are considered (all isotherms and all metadata). The other nine sets of results come from the combinations of isotherm culling (high, median, and low) and data culling (none, random 50%, and last 10%). To isolate the performance of the models, a logarithmic stress parameter function is chosen for all. The NMSE values are calculated with respect to the full dataset. A full assessment is performed for the LMP model, while an abridged assessment is performed for the other seven models.

Step 1: Import Creep Rupture Data. The raw dataset is composed of $N = 1300$ creep rupture data points. After disregarding the data points without the essential data and performing the isotherm merging, the raw dataset is reduced to $N = 1145$. This is the full dataset and will be used as the standard against which the accuracy of the other models will be evaluated. A plot of creep rupture for the full dataset is shown in Figure 7.

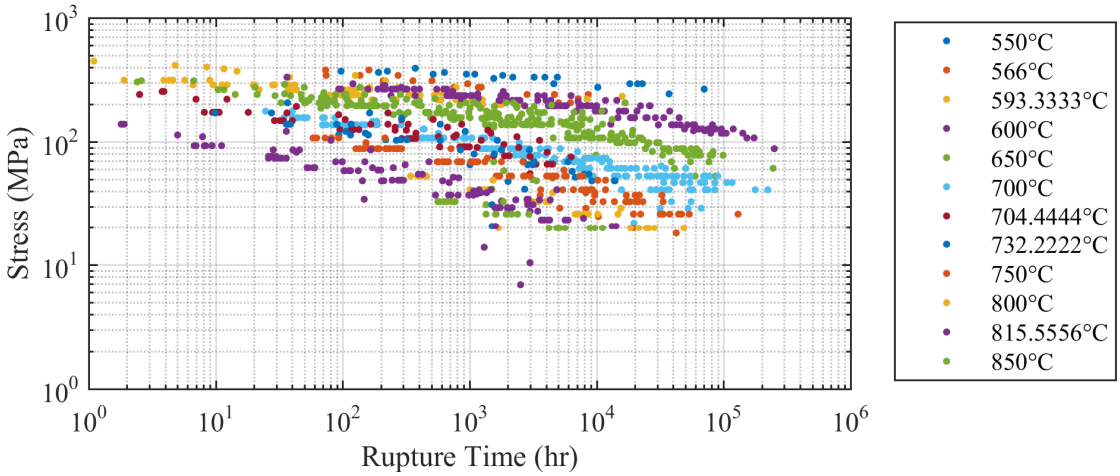

Figure 7 – Creep rupture, full dataset

Step 2 & Step 3: Cull by Isotherm & Simulate Limited Data. The full dataset is culled to consider the highest, median, and lowest isotherm. For each of these subsets, the main and supplementary temperatures are: $850\,°C$ and $815.56\,°C$; $700\,°C$ and $650\,°C$; $550\,°C$ and $566\,°C$. The supplementary isotherms are culled by 1/3 and the final isotherm datasets are shown in Figure 8. From here, the isotherm datasets are culled according to the three culling conditions.

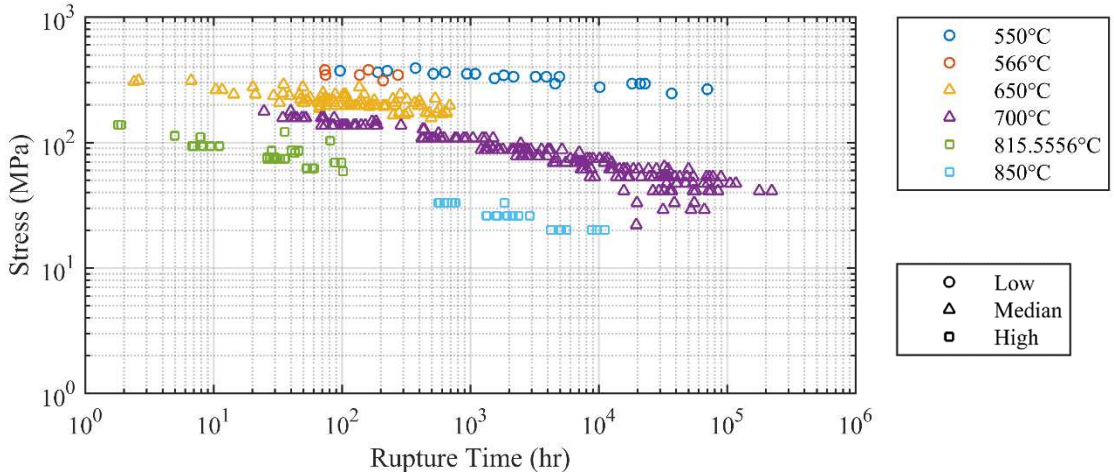

Figure 8 – Creep rupture, isotherm datasets

Step 4a: Creep Rupture Predictions, Full Dataset.

Creep rupture prediction for the full dataset are identical to those shown in Figure 4(a).

Step 4b: Creep Rupture Predictions, Culled Datasets. Isotherm and data culls are performed according to the guideline. First, the stress parameter functions for the cull conditions are discussed, followed by creep rupture predictions. The number of data points for each of the cull conditions are listed in Table 12. The material constants for the nine cull conditions using the LMP model are listed in Table 13. It is observed that the material constants for the nine cull conditions in Table 13 vary with respect to the nominal constants obtained for the full dataset. For instance, the high isotherm cull condition exhibits two instances of non-realistic material constants; when the data cull is Random 50% and Longest 10%, the material constant takes the value $t_a = -1.96$ and $t_a = -2.19$ respectively. The LMP material constant t_a is not supposed to be negative, so the creep rupture predictions made under these cull conditions should be scrutinized. The material constants for the median isotherm cull condition appears to come closest to the full dataset material constants, regardless of data cull.

Table 12 – Number of data points N per cull condition

	None	**50%**	**10%**
Low	27	17	24
Median	273	182	254
High	62	50	59

Table 13 – LMP material constants for cull conditions

Isotherm Cull	Data Cull	t_a	a_0, a_1, a_2
High	None	1.68	8467, -5.16, -2889
High	Random 50%	-1.96	4687, -7.22, -2377
High	Longest 10%	-2.19	4303, -7.75, -2248
Median	None	12.28	15600, -6.51, -2109
Median	Random 50%	11.28	15460, -4.94, -2471
Median	Longest 10%	11.92	14970, -6.84, -1908
Low	None	27.55	18396, -10.66, 842
Low	Random 50%	37.52	40219, 2.18, -7288
Low	Longest 10%	26.98	22891, -6.96, -1562

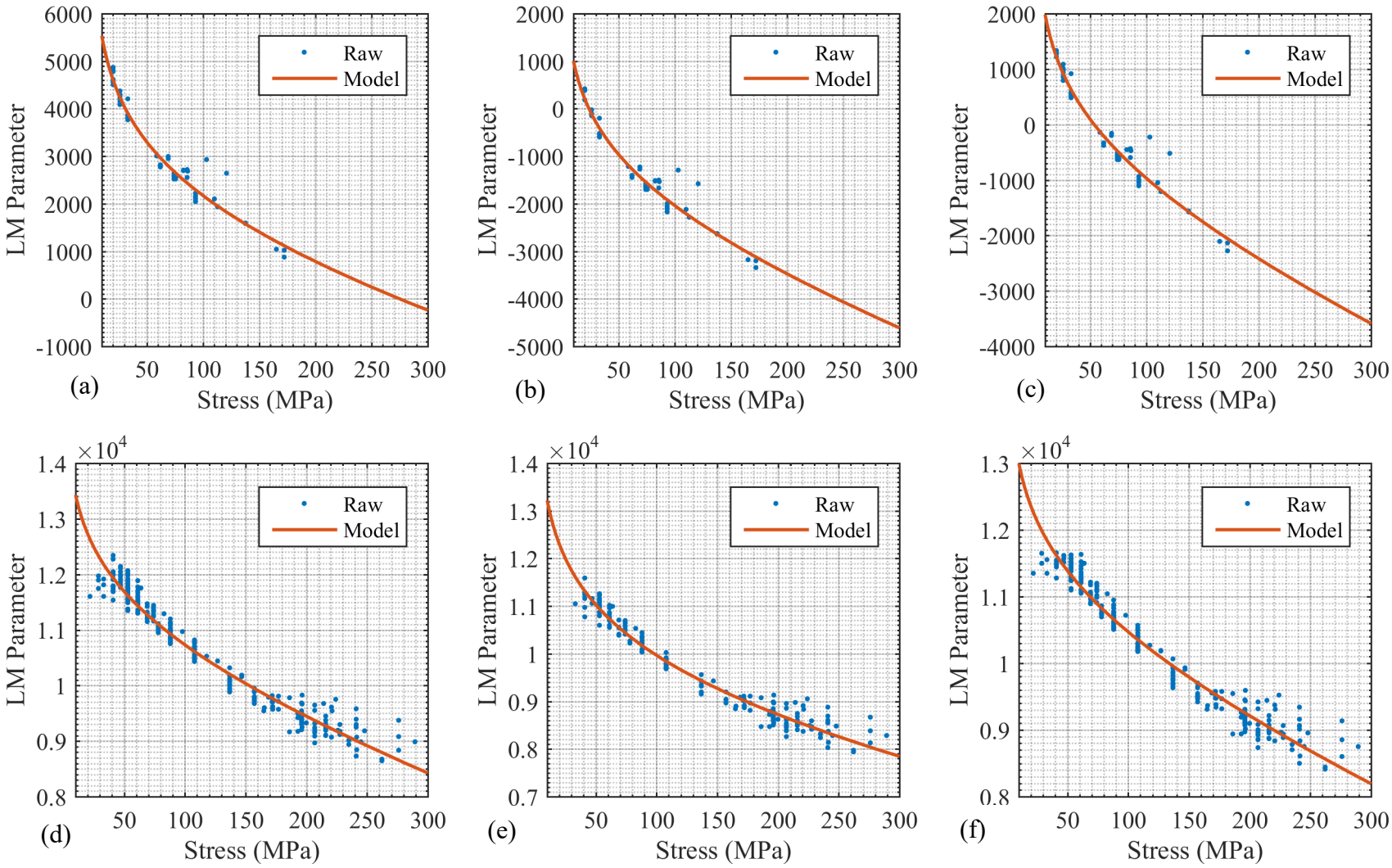

Figure 9 – Larson Miller stress parameterization: (a) high isotherm, no cull (b) high isotherm, 50% cull (c) high isotherm, last 10% cull (d) median isotherm, no cull (e) median isotherm, 50% cull (f) median isotherm, last 10% cull

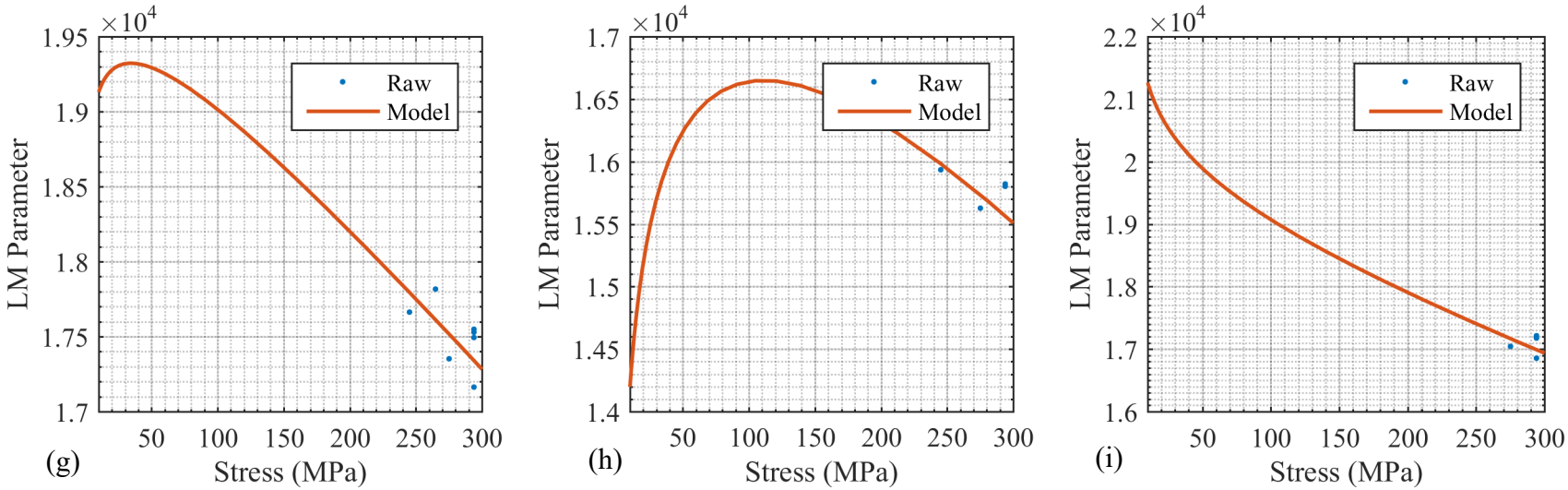

Figure 9, cont. – Larson-Miller stress parameterization (g) low isotherm, no cull (h) low isotherm, 50% cull (i) low isotherm, last 10% cull

First, the stress parameter function of the nine cull conditions are discussed; plots of these stress parameter functions are shown in Figure 9(a)-(i) for the LMP model. Most of the stress-parameterizations appear to give reasonable results in that the curves are positive and do not have an inflection point. However, there are several exceptions. The curves produced from high isotherm culling combined with Random 50% and Last 10% data culling (Figure 9(b) and Figure 9(c) respectively) show LMP values that are negative. They begin at approximately 20 MPa and 100 MPa for the Random 50% and Last 10% culling conditions, respectively. The curves produced by the low isotherm culling combined with None and Random 50% data culling (Figure 9(g) and Figure 9(h) respectively) show inflection points in the LMP curve. Stress parameterization curves that turn back like this can ultimately produce unrealistic creep rupture predictions. Using these stress parameterizations, creep rupture predictions are made for all nine culling conditions and are shown in Figure 10 through Figure 12.

(a)

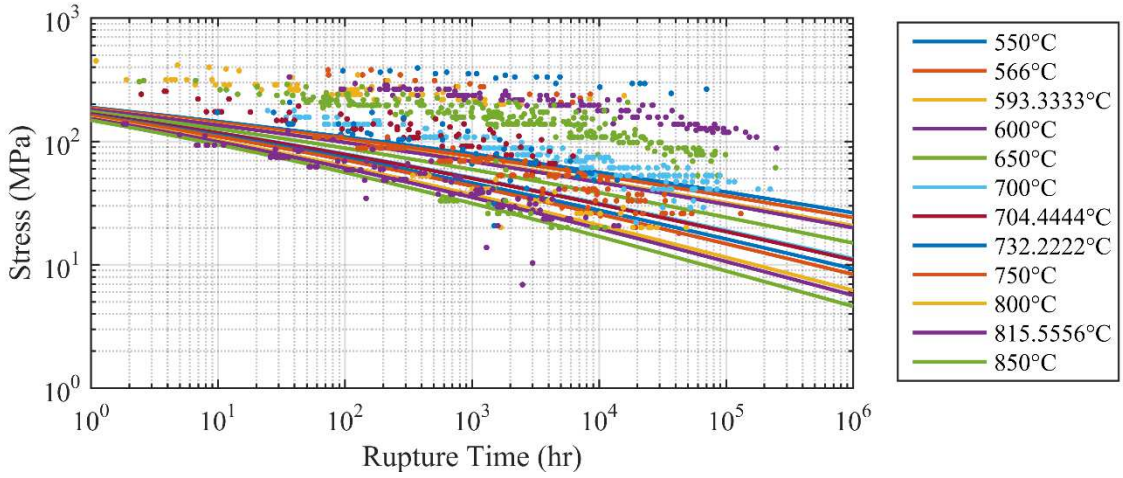

(b)

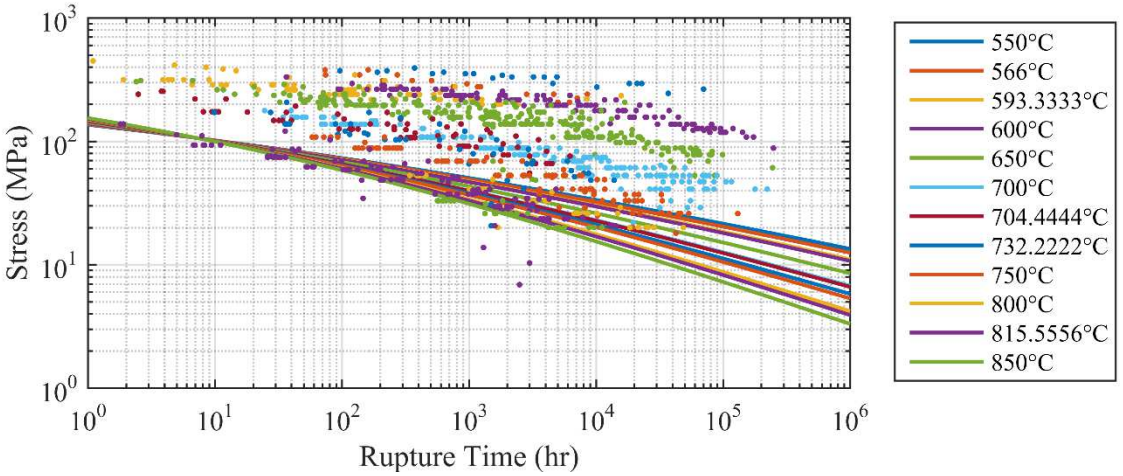

(c)

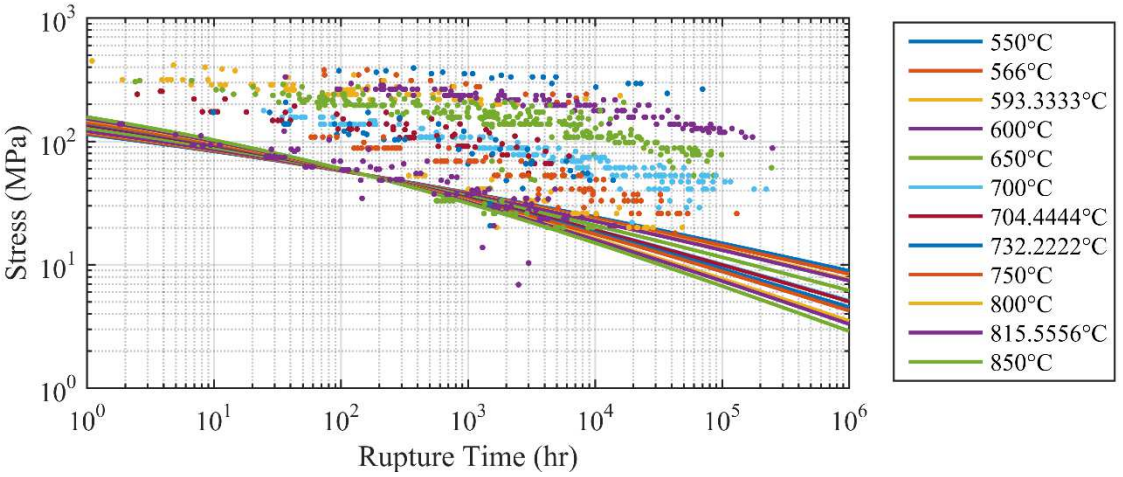

Figure 10 – LMP creep rupture predictions using high isotherm culling and (a) No cull (b) Random 50% cull (c) Last 10% cull

(a)

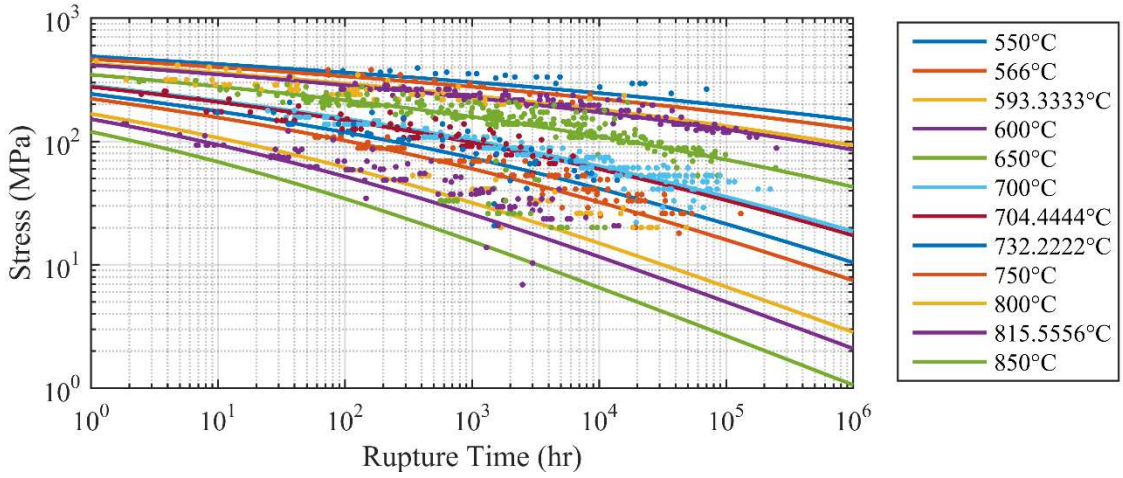

(b)

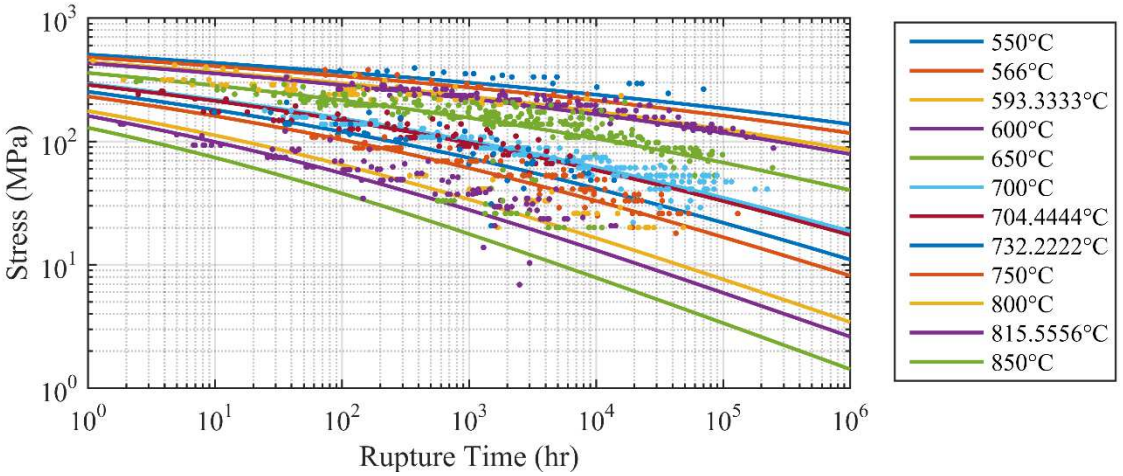

(c)

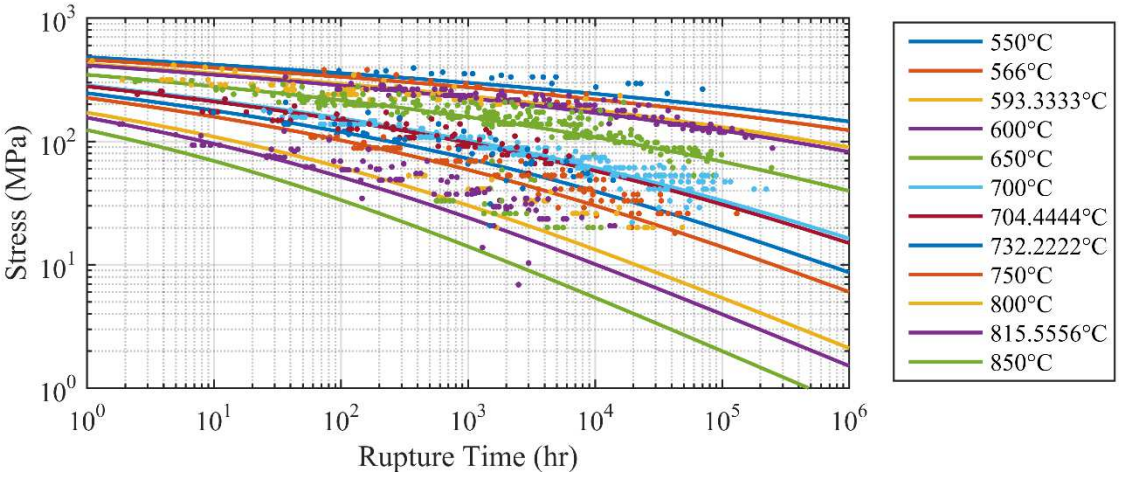

Figure 11 – LMP creep rupture predictions using median isotherm culling and (a) No cull (b) Random 50% cull (c) Last 10% cull

(a)

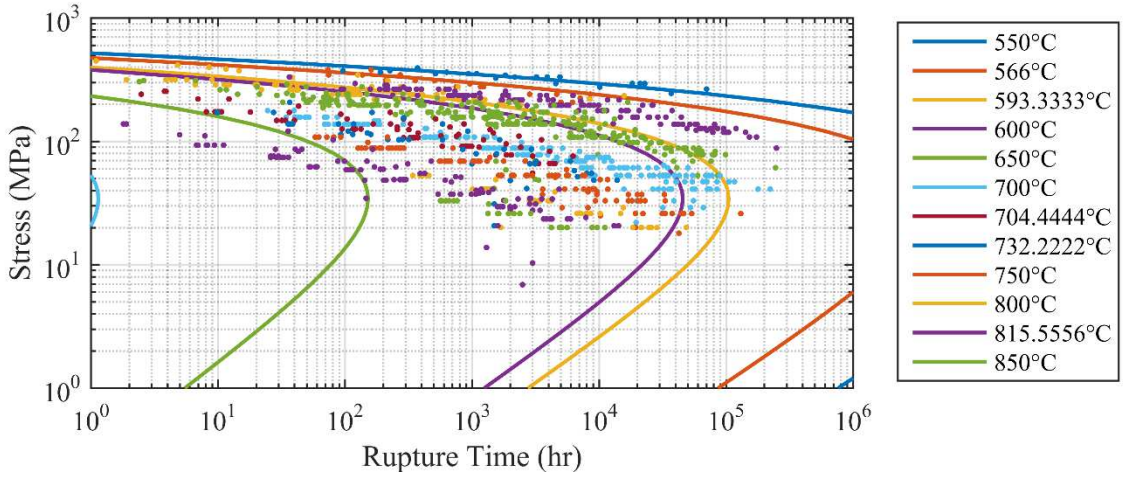

(b)

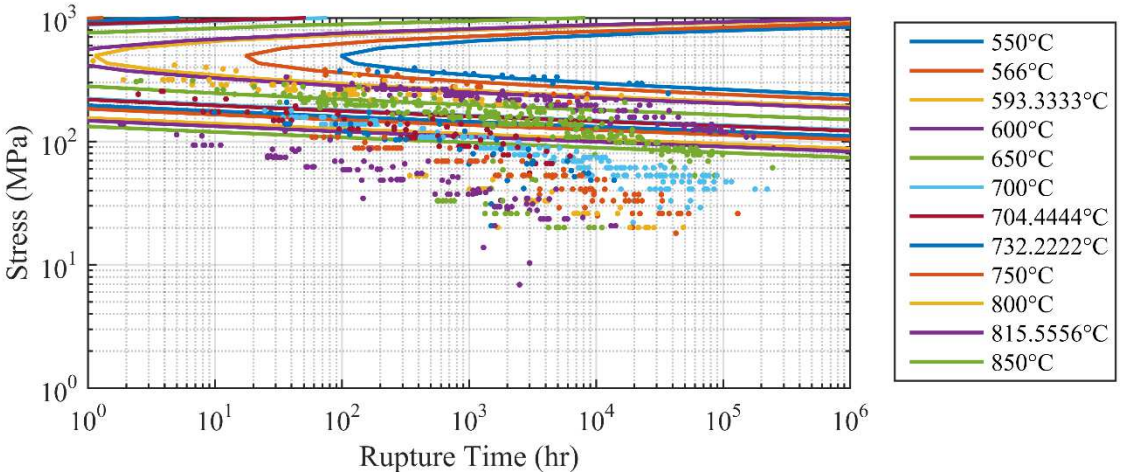

(c)

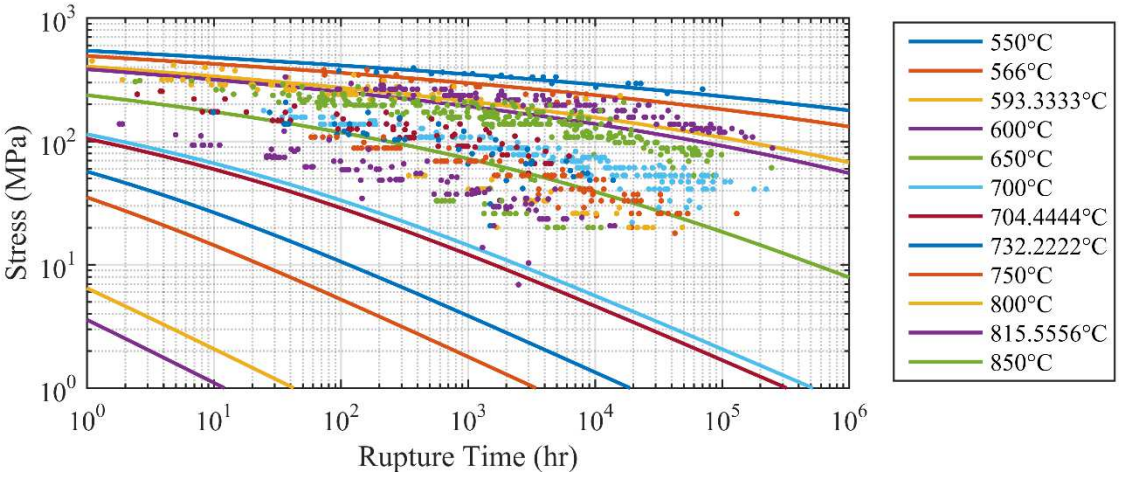

Figure 12 – LMP creep rupture predictions using low isotherm culling and (a) No cull (b) Random 50% cull (c) Last 10% cull

The creep rupture predictions for the high isotherm cull are shown in Figure 10(a)-(c) for No Cull, Random 50%, and Last 10% culling conditions respectively. The creep rupture predictions are not representative of the observed rupture for this isotherm cull, despite the having reasonably shaped stress-parameter curves. The creep rupture predictions are clustered near the isotherms used to make the predictions ($850\,°C$ and $815.56\,°C$), but are more closely clustered for the Random 50% or Last 10% culls. Performing no data cull produces isotherms that are more spread out than culling for either Random 50% and Last 10%, but these predictions still are not representative of the observed rupture. In all cases, the isotherms are clustered together. However, introducing data culling changes the behavior of the predications. While still clustered and thus unrealistic, the predictions for Random 50% and Last 10% data culls become even more tightly clustered, and come together at approximately 20 MPa and 175 MPa respectively. This suggests that LMP may be sensitive to both isotherm culling and data culling.

The creep rupture predictions for the median isotherm cull, as seen in Figure 11(a)-(c), are drastically different than the high isotherm cull. The prediction lines are not clustered around the isotherms used for the predictions ($650\,°C$ and $700\,°C$) and there are no inflection points. Data culling does not appear to have a significant effect on the creep rupture predictions. However, the prediction lines for the highest and lowest isotherms ($850\,°C$ and $550\,°C$) do not pass through all their respective observed creep rupture. This behavior was also observed when considering the full dataset, subject to no cull conditions. To assess the performance of these isotherm and data culling conditions, it is instructive to look at the NMSE values for each isotherm and compare them to those of the full dataset.

The creep rupture predictions for the low isotherm cull, as seen in Figure 12(a)-(c) are not representative of the observed rupture. Like the high isotherm cull, creep rupture predictions are

clustered near the isotherms used to make the predictions (550 °C and 556 °C), although not nearly as tightly. There are inflection points in the creep rupture predictions for No Cull and Random 50% culling conditions. Recall that the LMP stress parameter curve shows inflection points for this isotherm cull, so it was expected that the creep rupture predictions would also show inflection points. The implication of these predictions is that the LMP model appears to be heavily influenced by isotherm culling, whether it is high or low.

Step 5: Evaluate Physical Realism

In this section, the physical realism of the model is checked against the conditions listed in Table 5. These conditions are checked for the full dataset, metadata subsets, and the isotherm and data culls.

Zero-Stress Condition. At zero stress, the model should approximate creep rupture to be infinity. For the LM model, this can be determined analytically by looking at the stress-parameterization and rupture prediction equations ([Eq. (2)] and [Eq. (3)] respectively). At a value of $\sigma = 0$, the logarithmic stress-parameter equation can be approximated as negative infinity

$$\lim_{\sigma \to 0} \log(\sigma) = -\infty \tag{7}$$

If this is plugged into the rupture prediction equation, then rupture time is approximately zero, which is an unrealistic result. However, when the coefficient a_3 in [Eq. (2)] is negative, then the stress parameter equation becomes positive infinity, which is what the zero-stress condition requires. Thus, the validity of the zero-stress condition is dependent on the a_3 coefficient of the stress-parameter function

$$t_r = \begin{Bmatrix} \infty & if & a_3 < 0 \\ 0 & if & a_3 > 0 \end{Bmatrix} \tag{8}$$

As seen in Table 13, values of a_3 are negative for all nine cull conditions except for low isotherm, No Data cull. This indicates that the zero-stress condition is usually met when using the LM model and a logarithmic stress-parameter function.

Compressive Stress Condition. For compressive stresses ($\sigma < 0$), creep rupture should be approximately infinite. Unfortunately, a logarithmic stress-parameter function is undefined for negative values, which makes it an inadequate choice for assessing physical realism. However, this can be overcome by using a step function that returns zero is the stress is negative; such an equation is shown in [Eq.(9)].

$$t_r = \begin{Bmatrix} 0 & if & \sigma \le 0 \\ 10^{f(\sigma)/T + t_a} & if & \sigma > 0 \end{Bmatrix} \tag{9}$$

Ultimate Tensile Stress Condition. At the material's ultimate tensile strength (UTS), creep rupture should be approximately zero. However, UTS is a function of temperature. A plot of UTS vs. temperature is shown in Figure 7. Multiple temperature and stress conditions should be simulated to determine if the model is representative of material behavior. In this study, the simulated temperatures are $25\,°C$, $450\,°C$ and $920\,°C$ with UTS corresponding to 580 MPa, 430 MPa, and 83 MPa respectively. As seen in creep rupture predictions for these combinations and stress and temperature are performed for the nine cull conditions and are shown in Figure 14. For this analysis, rupture times below 1E-3 are considered to be zero and rupture times above 1E8 are considered infinite.

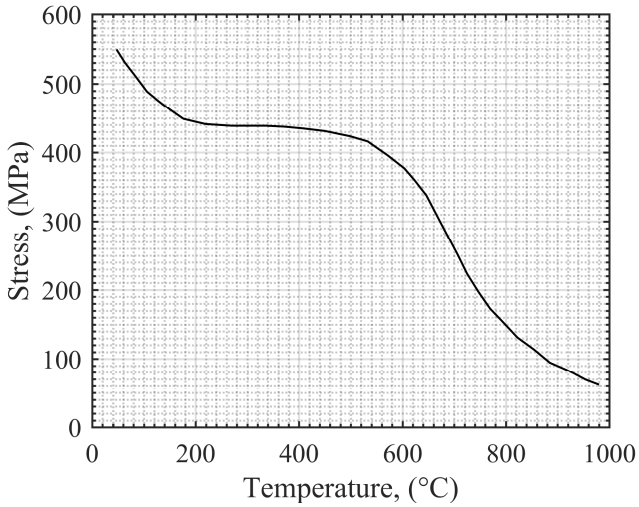

Figure 13 – UTS as a function of temperature for steels

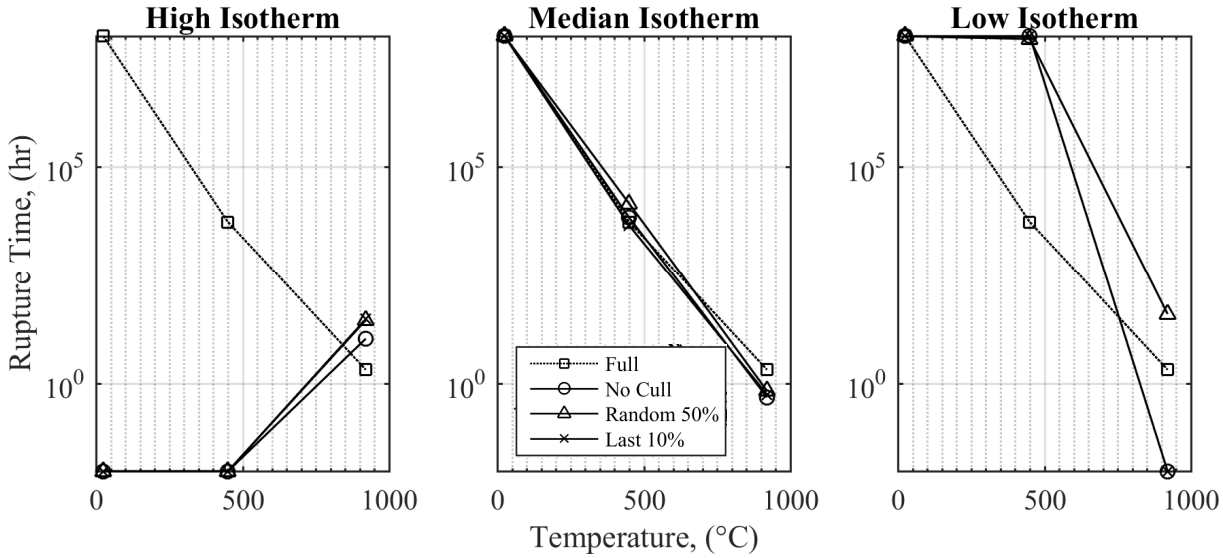

Figure 14 – Physical realism for UTS

For the high isotherm cull, it is observed that the rupture predictions do not agree with the actual response of the material. The UTS for $25\,°C$ and $450\,°C$ are approximately zero, but not for $920\,°C$, which shows an appreciable rupture time value. As temperature increases, the rupture prediction becomes larger by several orders of magnitude. The median isotherm cull, regardless of data cull, does not agree with the material response. Creep rupture times are approximately

infinite at 25 °C and do not approach zero, even at the highest temperature. For the low isotherm cull, creep rupture predictions are again inconsistent with the material behavior. However, at the highest temperature, creep rupture predictions approach zero for the No Cull and Last 10% cull conditions. In general, the LM model does not accurately predict rupture predictions for the ultimate tensile strength of 316SS.

Absolute Melting Temperature Condition. At the absolute melting temperature, creep rupture for steels should be zero. Creep rupture predictions for the LM model are made for each of the nine cull conditions and the full dataset. These predictions cover stress from 10 MPa to 1000 MPa. Stress rupture prediction at the absolute melting temperature are presented in Figure 15.

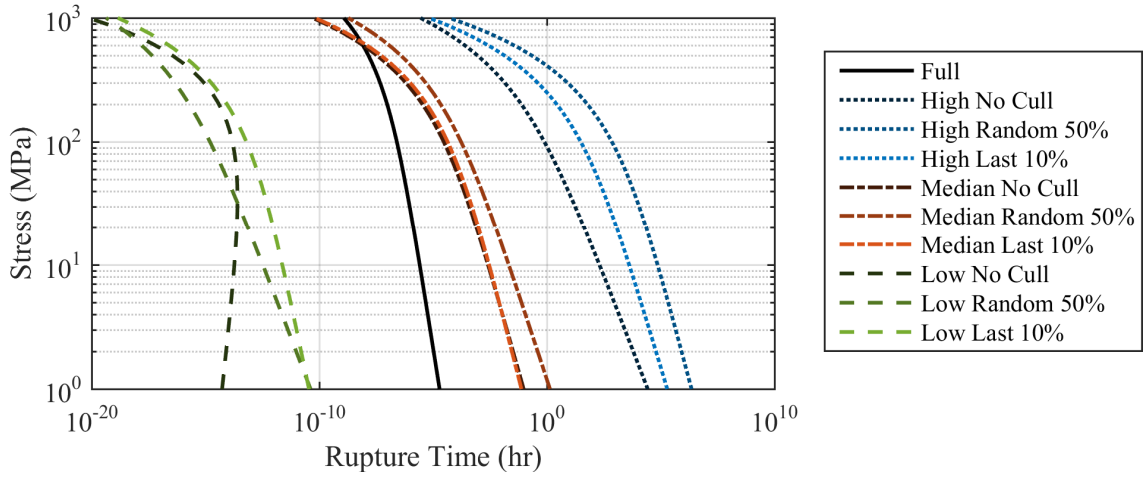

Figure 15 – Physical realism for absolute melting temperature, T_m

It is observed that the rupture predictions made with the full dataset show very small creep rupture predictions. As the isotherm and data culls change, the physical realism of the LM model changes significantly. For the low isotherm cull, no rupture time is predicted to be larger than 1E-10, which indicates this temperature cull is physically realistic. The median isotherm shows rupture times that are orders of magnitude larger than the low isotherm cull, but are still physically realistic for large stress values. The high isotherm, however, is the least physically realistic. Rupture times

approach 1E6 at low stresses, but are small for large stresses (larger than 500 MPa). It can be concluded that the physical realism of absolute melting temperature is dependent on the isotherm cull that is applied.

Accuracy of All TTP Models

For brevity, the full analysis of each model is not performed; only an abridged analysis wherein the NMSE values of each model are used to assess their predictive accuracy. The NMSE values of each of the eight models—subject to the nine culling condition—are illustrated graphically as 3D bar plots, shown in Figure 16(a)-(h). The raw NMSE values are listed alongside the bar plots in Table 14(a)-(h). For the bar plots, the isotherm and data culls are categorical values on the X-Y plane and the height of the bar represents the value of the NMSE for a given cull. For visual clarity, NMSE values larger than 3000 are clipped from the figures.

(a)

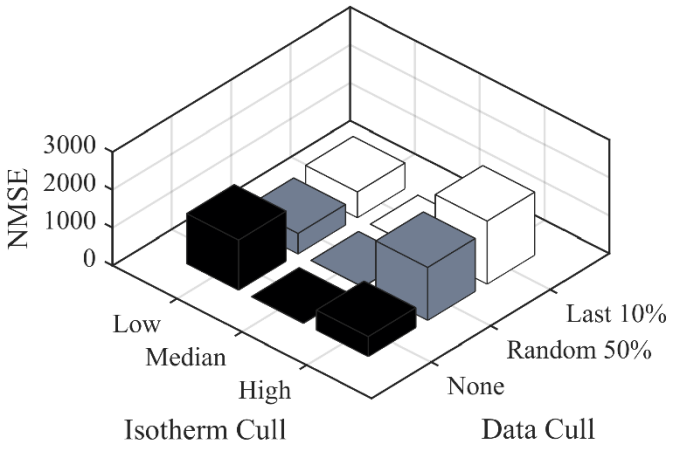

Table 14(a) – NMSE for cull conditions, LMP

	None	50%	10%
Low	1320	539	677
Median	3.00	2.11	2.84
High	525.71	1396	1662

(b)

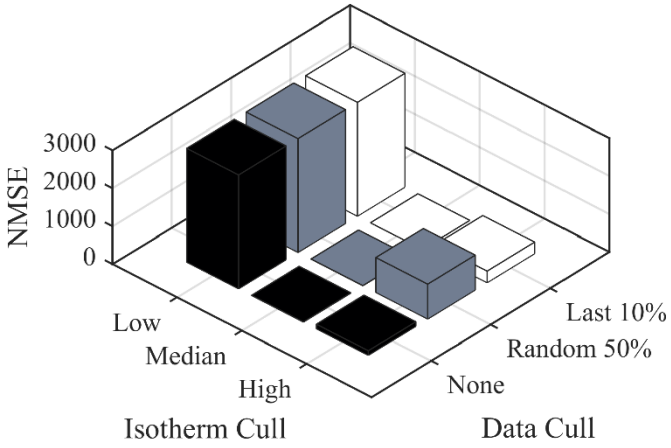

Table 14(b) – NMSE for cull conditions, MH

	None	50%	10%
Low	3668	3904	4244
Median	2.40	1.98	0.36
High	119.65	918.25	303.83

(c)

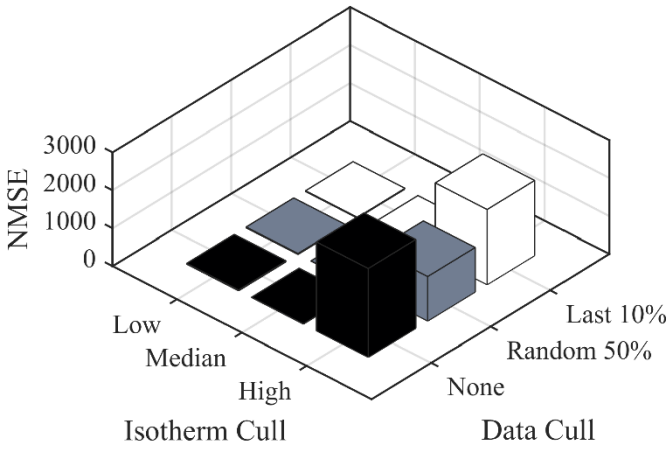

Table 14(c)– NMSE for cull conditions, MB

	None	50%	10%
Low	19.64	19.19	20.70
Median	4.28	6.09	4.69
High	2341	1155	1983

Figure 16 – NMSE values for full dataset using: (a) Larson-Miller (b) Manson-Haferd (c) Manson-Brown

(d)

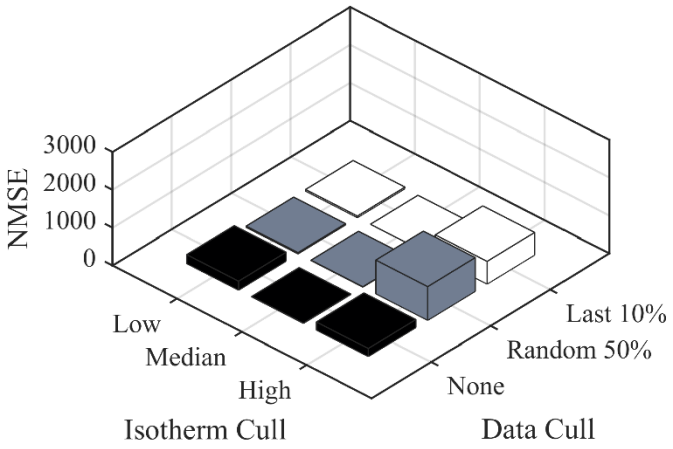

Table 14(d) – NMSE for cull conditions, OSD

	None	50%	10%
Low	234.46	31.47	40.95
Median	3.82	7.37	0.15
High	211.31	888.41	597.48

(e)

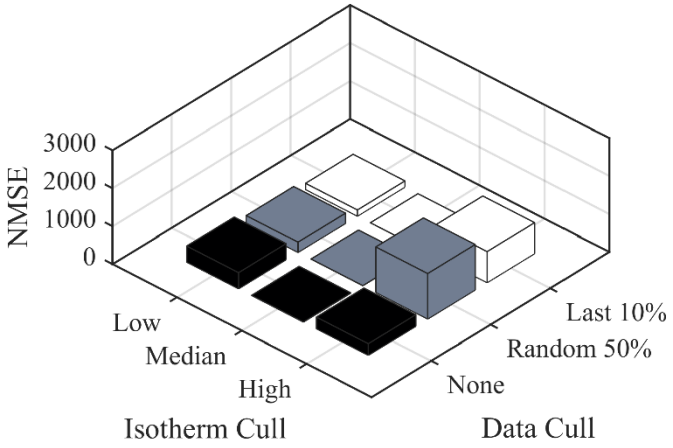

Table 14(e) – NMSE for cull conditions, MS

	None	50%	10%
Low	423.8	270.71	162.71
Median	1.39	1.21	1.46
High	306.7	1198	818

(f)

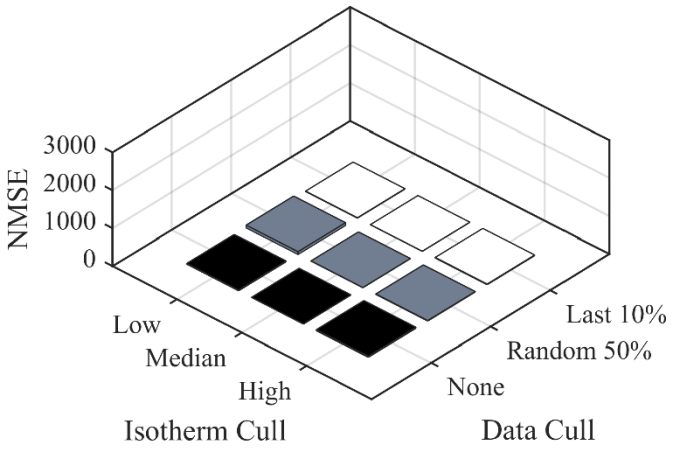

Table 14(f) – NMSE for cull conditions, GS

	None	50%	10%
Low	17.64	71.84	10.23
Median	2.44	4.54	4.86
High	27.95	11.47	16.61

Figure 16 – NMSE values for full dataset using (d) Orr-Sherby Dorn (e) Manson-Succop (f) Goldhoff-Sherby

(g)

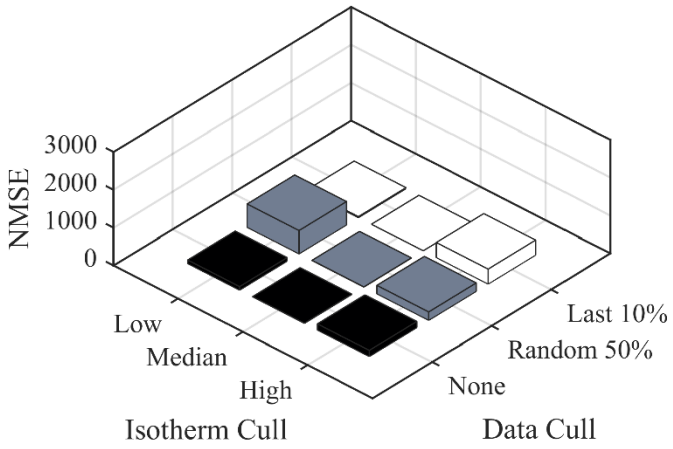

Table 14(g) – NMSE for cull conditions, MMH

	None	50%	10%
Low	92.05	616.25	26.04
Median	2.34	3.99	0.40
High	161.52	220.37	394.32

(h)

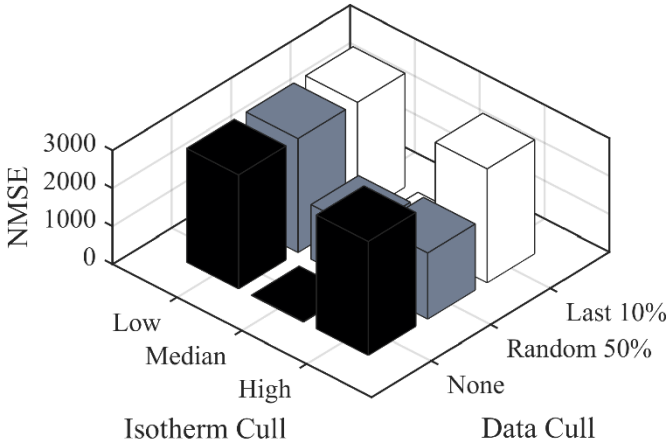

Table 14(h) – NMSE for cull conditions, MGW

	None	50%	10%
Low	Inf.	Inf.	Inf.
Median	7.36	1436	39.07
High	4164	1740	3622

Figure 16– NMSE values for full dataset using (f) Modified Manson-Haferd (g) Modified Graham-Wallace

It is observed some models are accurate regardless of which data cull and isotherm cull is chosen. The GS model shows low NMSE values for all cull conditions, where the largest NMSE is 27.95 for high isotherm and no data cull. The OSD, MS, and MMH models also show low NMSE values for all cull conditions. The poorest performing model appears to be MGW; the low culling condition produced NMSE values equal to infinity. However, the median isotherm cull for MGW are reasonably small, except for the 50% cull.

Across all models, a pattern is observed where culling for the median isotherms produces small NMSE values. This is especially noticeable for the MGW model, where NMSE values for

the low isotherm cull are close to infinity but are relatively small for the median isotherm cull. Even for models that showed low NMSE values across all cull conditions (such as GS), the median isotherm still produced the smallest NMSE. This indicates culling for the median isotherm—regardless of choice of model or data cull—produces more accurate predictions.

Conclusion

In conclusion, a guideline to assessing the statistical uncertainty of creep rupture databases and TTP models has been developed and is applied to 316SS. Limiting the amount of data used for creep rupture predictions can dramatically alter the accuracy of the extrapolations. The algorithm developed for this assessment enables flexible and rapid analysis of the performance of a model for a given material. There are several considerations in applying this assessment:

- The full dataset and its metadata subsets are adequately represented by LM model, but do not fully satisfy the criteria of ECCC standards of creep rupture predictions. There are large variations in the accuracy of the isotherms of the full dataset, which are not wholly dependent on data scatter. A visual analysis of the model is deceptive and one should instead rely on the descriptive statistics of a dataset.
- Isolating the temperature dependence of the TTP models produces dramatic differences in the accuracy of rupture predictions. Across all models, culling for the median isotherm often produced rupture predictions that agree well with predictions made by the full dataset. Culling for the low and high isotherm tended to produce unrealistic rupture predictions that clustered near the isotherms used for extrapolations. Culling for the low and high isotherm is therefore not recommended.

- Culling the number of data points also affects the accuracy of rupture predictions, but the differences are not as dramatic as culling by isotherm. Across most models, the Random 50% data cull gave less accurate rupture predictions than the Last 10% data cull.
- The physical realism of the LM model is mostly dependent on choice of stress-parameter function. A logarithmic function performed well for all conditions except for the Zero Stress and Negative Stress conditions.
- Several models performed well in terms of accuracy, regardless of culling conditions. For 316SS, the top three models are Orr-Sherby Dorn, Goldhoff-Sherby,and Modified Manson-Haferd.

Future Work

Future work should focus on performing a full analysis on all models, as was done for Larson-Miller. Additionally, the assessment of models should be reevaluated for stress parameter functions other than logarithmic. It is entirely possible that a stress parameter function exists that provides accurate creep rupture predictions regardless of data or isotherm culling. If possible, the assessment of models should be performed such that there are an equal number of data points for the three isotherm culls. In this way, the effect of data points on modeling may be removed from the assessment, which may help explain the anomalous accuracy that was seen for the median isotherm. Additionally, the effects of metadata on modeling should be examined for all metadata mentioned in this study.

Chapter 2: Accelerating the Acquisition of Creep Rupture Data

Introduction

Structural components in fossil energy (FE) power plants are designed to operate in the creep regime for a minimum of 300,000 hours [45]. The existing fleet has an average age of 40 years. The Department of Energy has outlined a strategy of life extension for US coal-fired power plants where many plants will operate as peakers for up to 30 additional years of service. It is possible that up to 613,620 hours of service could be accumulated in structured components in a FE power plant. There is a lack of experimental data and knowledge concerning creep behavior at this long time scale.

Conventional approaches to design against creep deformation and rupture involve the long-term creep testing of multiple specimens. Depending on the expected service conditions and service life of a component, a single creep test can take up to and beyond 100,000 hours. To truly characterize the creep resistance of a material, many combinations of stress and temperature must be tested so that constitutive and life prediction models can be calibrated. The National Science and Technology Council recognizes that the combination of the quantity, duration, and cost of creep testing makes the average time to implementation of a new high temperature alloy between 10 and 20 years [47]. The United States Department of Energy has emphasized that traditional materials operating in extreme thermomechanical environments are the limiting factor in increasing the efficiency and output capacities in energy, security, industry, electronics, and other sectors [48].

Accelerated Creep Testing (ACT) is a well-established method to estimate the creep strain and rupture properties of alloys used in the power generation industry. ACT tests are conventional creep tests conducted at a higher temperature and/or stress, the results of which are extrapolated

to low temperature and/or stress conditions [49]. International codes such as the ASME B&PV III, French RCC-MR, and British R5 recommend a phenomenological approach to creep and creep-fatigue where short-term creep data is extrapolated to long-term using predictive models, regression analysis, and confidence bands to manage reliability and preserve conservatism [50-53].

The extrapolation of ACT data to predict low stress and temperature rupture is performed using predictive models. Master curve models are the most commonly employed, where the relationships between stress, temperature, rupture time, minimum creep strain rate, and/or creep deformation are parameterized onto a single curve. In master curve models, the isotherms of creep can be collapsed onto a single curve, that when plotted as a function of stress enables predictions of the rupture time at any stress and temperature condition. The "classic" and most commonly applied models are Larson-Miller, Orr-Sherby-Dorn, and Monkman-Grant [55-57]. The Larson-Miller and Orr-Sherby-Dorn models correlate applied stress to temperature and creep rupture, while Monkman-Grant correlates minimum creep rate to creep rupture. Master curve models are favored for their ability to predict long-term creep rupture using short-term creep rupture data; however, to calibrate the extrapolation, a sufficient number of midrange stress and temperature creep tests must be performed to ensure the extrapolated creep rupture predictions are representative of actual material behavior. In addition, conventional master curve models have a limited ability to predict multistage (primary, secondary, and tertiary) creep deformation. For ACT to be valid, care must to be taken to:

- Simulate the service failure mode,
- Remain in a single deformation mechanism zone,
- Produce a realistic oxidation state,

- Replicate the metallurgical instabilities that develop at the target boundary conditions.

The stepped isothermal method (SIM) and stepped isostress method (SSM) are newly developed ACT tests (designed for polymers) that provide not only creep-rupture prediction, but also the multistage creep deformation at any desired stress and temperature. The SIM and SSM are creep tests where multiple stepped increases of temperature or stress are applied at a fixed interval. After testing, the SIM and SSM data are strain- and time-adjusted according to the time-temperature (TTSP) and time-stress superposition principle (TSSP) [59-70]. Each test results in a single accelerated creep deformation curve that includes rupture if the SIM or SSM test ruptured during testing. In general, SSM is the preferred method because local load control offers tighter PID control (less variations) and can be step-changed more quickly when compared to temperature control.

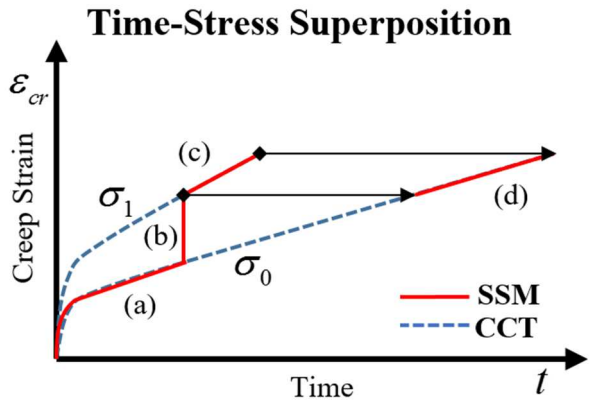

Figure 17 – Time-Stress Superposition Principle visualization of (a) reference stress (b) stress step (c) elevated stress level (d) accelerated creep strain for the reference stress

The SSM approach uses the time-stress superposition principle (TSSP) to accelerate creep deformation and rupture life at a reference stress level. According to TSSP the rate-dependent properties of a viscoplastic material at a reference stress level is equivalent to a time-shifted strain response at an elevated stress level, as depicted in Figure 17 [61]. This relationship is shown below:

$$\varepsilon_{cr}\left(\sigma_0, t\right) = \varepsilon_{cr}\left(\sigma_1, {}^{t}\!/\!_{\phi}\right) \tag{10}$$

where ε_{cr} is creep strain, t is time, σ_0 is the reference stress, σ_1 is an elevated stress, and ϕ is the time shift factor for the elevated stress.

The creep-rupture and deformation curves acquired with SSM consistently agree well with those obtained using SIM and conventional creep tests (CCTs). A set of 24 hr SSM tests for aramid fibers were accelerated to 104 hours for high stresses and 107 hours for low stresses [62, 65, 66]. A 30 hr SSM test for polyamide 6 thermoplastic was accelerated to nearly 2.4×106 hr [68]. A 15 and 30 hr set of SSM tests for CFRPs were accelerated to approximately 30 and 300 hr respectively [26]. A 12 hr set of SSM tests for Bibolo wood were accelerated to 1.67×1015 hr [69].

There are several issues to consider in applying the SSM procedure. To the authors' knowledge, the SSM approach has only been applied at room temperature. It is unknown if SSM works for metallics. There is no systematic approach in processing the SSM data to produce accelerated creep deformation curves. Specifically, laws to determine the virtual start time and mechanistic rules to determine the shift factors are not detailed in literature.

In this study, a new systematic approach to applying SSM is introduced. The feasibility of SSM for metallics will be assessed by applying the systematic approach to 304SS. The creep deformation and rupture will be post-audit validated by performing CCT and comparing the results. Conclusions concerning the capabilities and limitations of the SSM protocol will be discussed.

A Systematic Approach to the Stepped Isostress Method

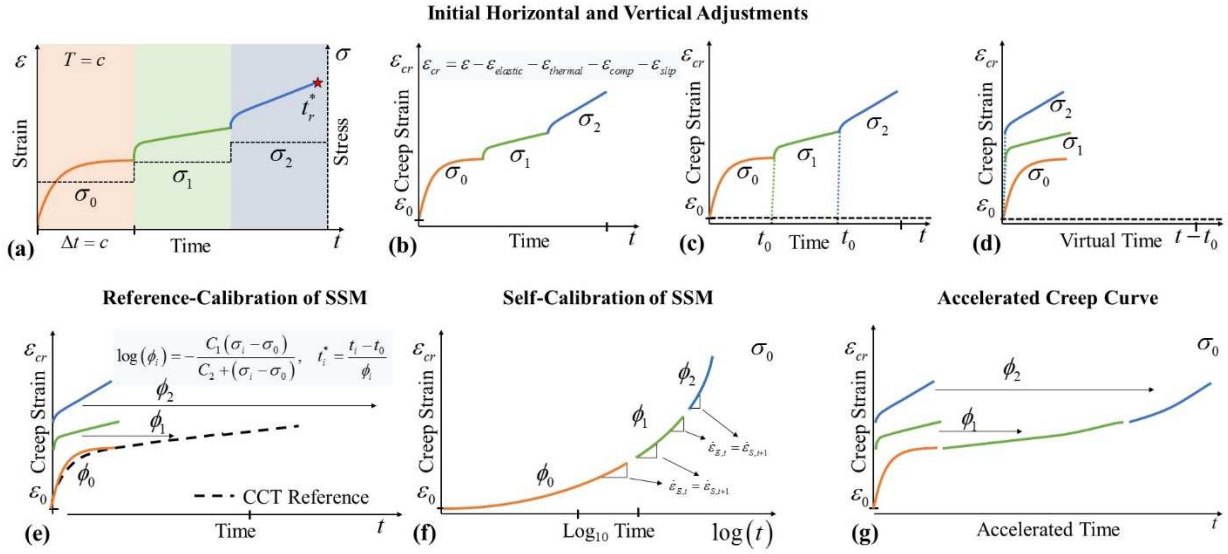

Figure 18 – Stepped Isostress Method (SSM) procedure (a) Total strain-time data (b) creep strain adjustment (c) extrapolation to zero strain (d) virtual start time adjustment (e) reference-calibration (f) self-calibration (g) accelerated creep curve.

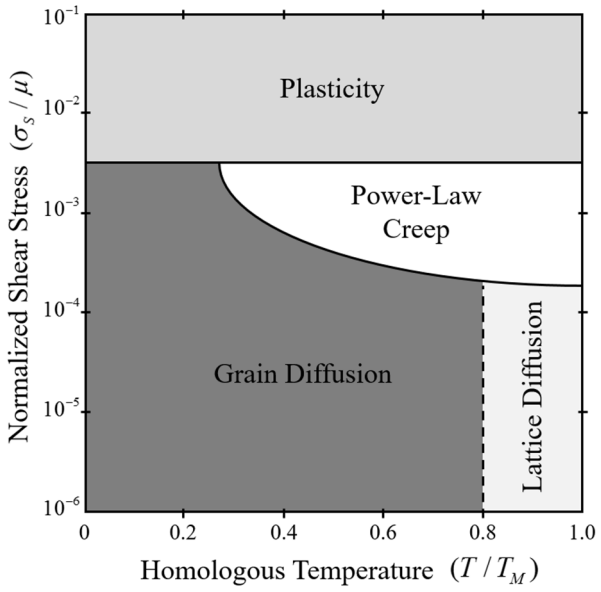

Figure 19 – Deformation mechanism map for 304SS

The new systematic approach to SSM includes the following features:

- Deformation mechanism maps are taken into consideration;
- A constitutive law to determine the virtual start time;

- A reference-calibration approach (Optional);
    - Mathematical rule for determine the time shift factors via short reference CCT.
- A self-calibration approach;
    - Mathematical rule for determining the time shift factors via creep strain rate matching between stress levels.

The procedure for the systematic SSM is illustrated in Figure 18. The steps to the approach are as follows:

Step 1: Selecting Test Conditions

For SSM to be valid, the applied stress levels σ_i, and temperature T, must remain within the boundaries of a single deformation mechanism. This can be ensured by selecting boundary conditions using a deformation mechanism map. A schematic of the deformation mechanisms for 304SS is provided in Figure 19. The stress level and temperature for the SSM procedure should be selected such that the specimen (i) does not transition between deformation mechanisms and (ii) does not remain on a mechanism transition boundary. Mixing deformation mechanisms during the SSM test will render the accelerated creep results invalid. It should be notes that these boundary condition restrictions limit the maximum acceleration ability of SSM. The larger the stress steps, the greater the acceleration ability. By limiting the available stress range, acceleration is capped. Ideally the **magnitude of stress steps,** $\Delta\sigma$ **should be** maximized yet offer **enough space for 3 stress steps** (4 total stress levels) to be performed inside the boundaries of the given deformation mechanism.

Step 2: Perform CCT Tests

The CCTS are used to determine the minimum hold duration, Δt of the SSM. The hold duration is fixed for all stress levels and should be long enough for the minimum creep strain rate (secondary creep regime) to be reached at the reference stress level.

Optionally, the CCTs can be used to calibrate the time-shift factors (reference-calibration). The CCT duration should be long enough for the accumulated creep strain of the CCT to exceed the accelerated creep strain of the first two stress levels in the planned SSM. This requires that the SSM test be performed first. The accumulated creep strain at the end of the first two stress levels becomes the stopping criterion for the CCT. Since the amount of acceleration of the SSM is not known a priori, it is difficult to determine the CCT duration without testing. Once an adequate CCT is obtained, the time-shift factor of the SSM can be calibrated by numerically minimizing the error between the CCT and SSM creep deformation curve as depicted in Figure 18e. Due to the lack of knowledge concerning lack of CCT duration, this is not the preferred method of calibration. An alternative self-calibration approach will be presented later.

Step 3: Perform SSM Tests

The isotherm SSM tests are started at a reference stress level and are stepped through increasing stress levels with a fixed magnitude at a fixed hold duration. A schematic of the stress and strain history is shown in Figure 18a. The magnitude of stress steps should be maximized within the limits of the target deformation mechanism (details in Step 1). The hold duration should be minimized but encompass the minimum creep strain rate at the reference stress level (details in Step 2). The final stress level should be maintained until rupture. The duration of the transitions between stress levels should be as short as possible while avoiding shock forces.

Step 4: Execute Systematic Adjustments to Produce Accelerated Creep Data

The systematic SSM procedure should be written as a self-contained program in a programming language. Each SSM adjustment should be a subroutine in the program. Minimal manual modification or manipulation of the SSM data should be performed to mitigate subjectivity.

Step 4a: Creep Strain Adjustment

During SSM, the total strain, ε is recorded as depicted in Figure 18a. The total strain, ε must be rearranged to calculate the creep strain, ε_{cr} as follows

$$\varepsilon_{cr} = \varepsilon - \varepsilon_{elastic} - \varepsilon_{thermal} - \varepsilon_{comp} - \varepsilon_{slip} \tag{11}$$

where $\varepsilon_{elastic}$ is the elastic strain, $\varepsilon_{thermal}$ is the thermal strain, ε_{comp} is the machine compliance strain, and ε_{slip} is the extensometer slip strain. This will produce the creep deformation curve observed in Figure 18b. The type, method, and root cause of each strain is described in Table 15.

The elastic and thermal strain can be removed mathematically using the following relations

$$\varepsilon_{elastic} = \frac{\sigma(t)}{E\left(T\left(t\right)\right)} \tag{12}$$

$$\varepsilon_{thermal} = \alpha\left(T(t) - T_0\right) \tag{13}$$

where $\sigma(t)$ is the applied stress as a function of time, $E\left(T\right)$ is the modulus of elasticity as a function of temperature, α is the coefficient of thermal expansion, $T(t)$ is temperature is a function of time, and T_0 is an arbitrary reference temperature. The machine compliance and extensometer slip strains must be manually identified and input into the program.

Table 15 – Breakdown of strain type, method, and root cause

Strain Type	Method	Root Cause
Elastic strain, $\varepsilon_{elastic}$	Calculated	The recoverable elastic deformation that occurs in the specimen upon stress change.
Thermal strain, $\varepsilon_{thermal}$	Calculated	The recoverable thermal deformation that occurs in the specimen upon temperature change.
Machine compliance strain, ε_{comp}	Manual Input	Strains due to interaction between elastic, thermal, and creep deformation in the specimen and testing equipment (crosshead, pull rods, threaded adapters, etc.). The machine compliance strain includes pre-load strains and anomalous strains observed at each stress step. Usually only observed in crosshead displacement data.
Extensometer slip strain, ε_{slip}	Manual Input	If the extensometer slips, an anomalous jump or drop in strain can be recorded and should be removed. A rare occurrence.

Step 4b: Virtual Start Time Adjustment

The *virtual start time adjustment* is applied to offset the creep deformation of each stress level by a virtual start time, t_0 as if each curve had been produced from an independent, initially unloaded creep test. The virtual start time, t_0 is obtained by fitting a constitutive law to each stress level and identify the time at which creep strain is equal to zero. This is illustrated in Figure 18c. The common method is to fit a 2nd order polynomial to the creep deformation. The polynomial is equivalent to the Graham and Walles constitutive law, $\varepsilon_{cr} = \sum a_i t^{n_i}$ where a and n are material constants and t is time. In general, the following rules must be enforced when selecting a constitutive model. The constitutive models must:

- be able to model primary, secondary, and tertiary creep. Ideally, the regimes should be separated into independent functions such that the model can be simplified to better fit the given stress level. For instance, if there is no tertiary creep regime at a stress level, the function associated with tertiary creep should be zeroed out to increase the statistical dependencies of the material constants for primary and secondary regimes.

- be able to predict zero strain at a non-zero time. In most cases, this can be introduced by replacing t with $(t-t_0)$ everywhere; however, care must be taken to prevent the constitutive model from becoming over-defined. Zeroing out unnecessary creep regimes can help mitigate this issue.

In this study, a modified Theta projection model is employed:

$$\varepsilon(t)=\theta_1\left(1-\exp(-\theta_2\cdot(t-t_0))\right)+\theta_3\left(\exp(\theta_4\cdot(t-t_0))-1\right) \tag{14}$$

where θ_1 and θ_3 scale the magnitude of the primary and tertiary creep strains respectively, θ_2 and θ_4 control the curvature of the primary and tertiary creep strains respectively, t is time, and t_0 is virtual time. The creep strain for each stress level is extrapolated to zero strain and the creep curves are shifted to a common reference start time of zero as illustrated in Figure 18d.

Step 4c: Time-Shift Adjustment

Finally, the *time-shift adjustment* is applied to time-shift the individual creep deformation curves to produce an accelerated creep deformation curve. The creep strain from each stress level is shifted in time with the phenomenological time-shift factor, ϕ_i, by Williams, Landel, and Ferry (WLF) equation:

$$\log(\phi_i)=-\frac{C_1(\sigma_i-\sigma_0)}{C_2+(\sigma_i-\sigma_0)},\quad \phi_i=10^{-\frac{C_1(\sigma_i-\sigma_0)}{C_2+(\sigma_i-\sigma_0)}},\quad t^*=\left(\frac{t-t_0}{\phi_i}\right); \tag{15}$$

where C_1 and C_2 are material constants, ϕ_i is the time-shift factor for the i^{th} stepped stress, σ_0 and σ_i are the reference stress and i^{th} stepped stress of the SSM test respectively, t^* is accelerated time, t is real time, and t_0 the virtual start time [[72]. The constant C_2 must be greater than zero.

Two methods for calibrating the WLF equation exist: the reference- and self-calibration approaches respectively. The reference-calibration approach is described in detail in Step 2. It is

not the preferred method. It is recommended that the self-calibration approach be applied in most cases. The self-calibration approach is based on creep strain rate matching between stress levels. In a typical creep deformation curve, the creep strain rate does not exhibit a dramatic change in rate but exhibits a continuous curve. The stress levels in the SSM approach do have a dramatic deviation in creep strain rate. Using the self-calibration approach, the C_1 and C_2 material constants of WLF [Eq. (15)] are adjusted until the error between the ending and beginning creep strain rates between stress levels is minimized. This will result in a continuous accelerated creep curve. This process is illustrated in Figure 18f. A mathematical description of this criterion is provided below:

$$\dot{\varepsilon}_{E,i} = \dot{\varepsilon}_{S,i+1}, \quad \frac{\Delta\varepsilon_{E,i}}{\Delta t_i^*} = \frac{\Delta\varepsilon_{S,i+1}}{\Delta t_{i+1}^*} \tag{16}$$

where $\dot{\varepsilon}_{E,i}$ is the ending accelerating creep strain rate of the i^{th} stress level, $\dot{\varepsilon}_{S+i}$ is the starting creep strain rate of the $i^{th}+1$ stress level, and t^* is accelerated time. During a typical creep test, the creep strain rate can fluctuate; therefore, it is recommended that the starting and ending strain rate be averaged over an hour of real time.

It is recommended that C_1 and C_2 be optimized using the normalized mean squared error, *NSME*:

$$NMSE = \frac{1}{n}\sum_{i=1}^{n}\left[\left(\dot{\varepsilon}_{E,i} - \dot{\varepsilon}_{S,i+1}\right)\Big/\dot{\varepsilon}_{MAX,i}\right]^2 \tag{17}$$

where $\dot{\varepsilon}_{MAX,i}$ is the larger of the starting or ending strain rates observed at the given step and *n* is the number of stress levels.

Experiments

To validate the new systematic approach works for metallics, SSM tests are performed on 304 stainless steel at 600°C. The SSM tests will be post-audit validated by performing CCT tests and comparing the results.

Materials and Specimen

The subject material of this study is rod-stock type 304 stainless steel (304SS), an austenitic Fe-Ni-Cr stainless steel. Specimens are prepared according to ASTM E8 and E139 [75, 76] with an overall length of 4.0 inches, a reduced diameter of 0.25 inches, and a gage length of 1.0 inch, as depicted in Figure 20. The typical chemical composition of 304SS is provided in Table 16. Type 304SS is a standard material used in structural applications that exhibits similar mechanical behavior and creep resistance to other alloys. Thus, if SSM tests work for 304SS, justification is provided for applying SSM to other metallics.

Table 16 – Chemical composition (weight %) of SS304 [[73]

	Fe	Cr	Ni	C	Mn	Cu	Mo	Si	S	P	Co	N
AVG	69	19	9.25	0.04	1	0.5	0.5	0.5	0.015	0.023	0.1	0.05

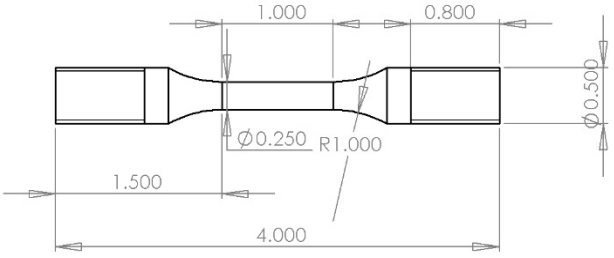

Figure 20 – Drawing of specimen (in inches)

Table 17 – Monotonic tensile properties of 304SS

	Tensile Strength, σ_{UTS} (MPa)	Yield Strength, σ_{YS} (MPa)	Modulus, E (GPa)	Elongation (%)
RT	662.00	396.33	108.51	80.51
600°C	344.00	199.03	104.47	42.29

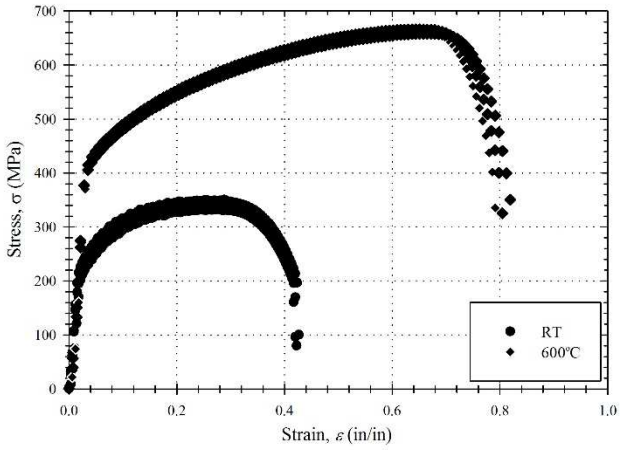

Figure 21 – Stress-strain curves of 304SS

Three monotonic tensile tests are performed on 304SS at room temperature and 600°C, conforming to ASTM E21 [77]. The resulting stress-strain curves are provided in Figure 21. The average ultimate tensile strength, 0.2% offset yield strength, modulus of elasticity, and elongation are listed in Table 17.

Equipment

Mechanical tests are conducted with an Instron 5969 universal test machine (50kN ±100N). An ATS Model 3210 split-tube furnace is used to heat the specimens with three vertically aligned heating zones. During high temperature tests, the target temperature is reached in approximately 25 min and maintained for 1 hr to allow for adequate soak time. An Epsilon Model 3448 high-temperature extensometer is used to measure displacement and strain. The contact rods of the extensometer are covered with flexible ceramic sleeves to prevent small disturbances caused by heat turbulence. A Type-K thermocouple is directly welded to the specimen to measure surface temperature. The Instron frame is centrally controlled by a desktop computer running the Bluehill Software (version 3.54) control system. Load, time, crosshead displacement, specimen extension, and temperature are recorded.

Stepped Isostress Method (SSM) and Creep Tests

Table 18 – Test matrix for SSM tests

Temp., T (°C)	Stress Levels, σ_i (MPa)	Magnitude of Stress Step, $\Delta\sigma$ (MPa)	Hold duration, Δt (hr)	Repeats
600	290, 292.5, 295, 297.5	2.5	5	2
600	280, 285, 290, 295	5	5	2

SSM test are performed according to the systematic approach detailed in Step 3. A test matrix of the SSM tests is listed in Table 18. Three elevated stress levels are carried out where the last stress level is held indefinitely until rupture. The transition time between stress levels is one minute. In total, four tests are performed.

Table 19 – Test matrix for CCT tests

Temp. (°C)	Stress (MPa)	Repeats
600	290	2
600	280	2

Conventional creep tests are performed according to ASTM E139 [76]. A test matrix for the CCTs is listed in Table 19. The CCT tests are performed to post-audit validate the SSM self-calibration approach. The creep tests are performed for a maximum of 168 hr (one week).

Results and Discussion

A detailed walkthrough of the systematic SSM data adjustment procedure is provided below for a SSM test conducted at a temperature of 600°C, reference stress of 290 MPa, and stress steps of 2.5 MPa each held for 5 hours. The last stress level is held indefinitely until material failure.

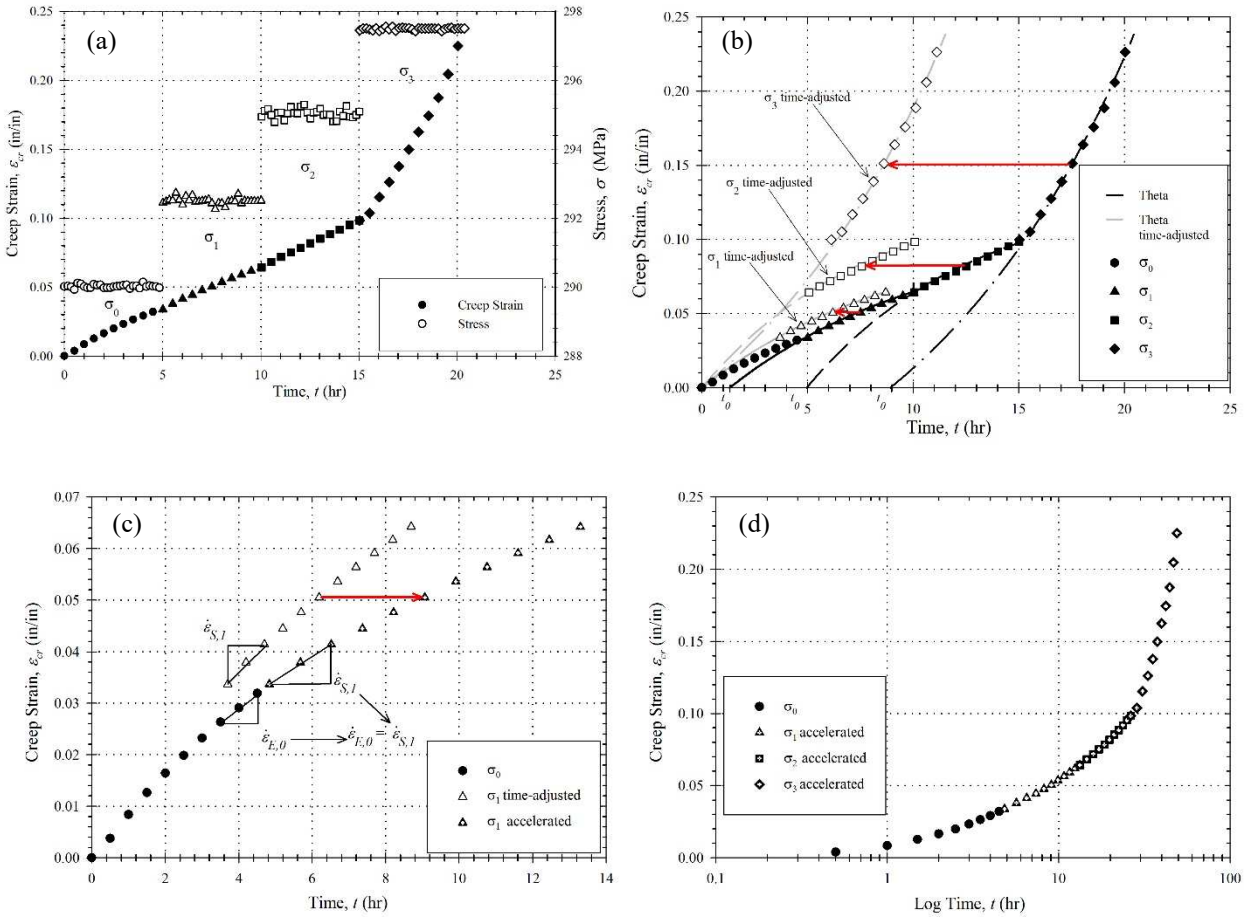

Figure 22 – Walkthrough of SSM procedure (a) Creep strain adjustment (b) Virtual start time adjustment (c) Self-calibration between stress levels (d) accelerated creep deformation and rupture

Table 20 – Material constants θ

Stress Level (MPa)	θ_1	θ_2	θ_3	θ_4
σ_1 = 292.5	0.109022	0.103578	0	0
σ_2 = 295.0	0.135966	0.125951	0	0
σ_3 = 297.5	0.052232	0.046376	0.08481	0.109931

The *creep strain adjustments* (Step 4a) are performed on the SSM strain data to produce a continuous creep deformation curve, as shown in Figure 22a. A creep ductility of 22.74% is observed.

The *virtual start time adjustment* (Step 4b) begins by fitting the Theta projection constitutive model to the creep strain of each stress level. A summary of the material constants θ_i for each stress level is provided in Table 20. The first two stress levels σ_1 and σ_2 are best represented by the primary and secondary creep regimes, thus only θ_1 and θ_2 are optimized. The last stress level, σ_3 is best represented by all three creep regimes; therefore, θ_1, θ_2, θ_3, and θ_4 are optimized. Once the Theta models are fit to the experimental data, virtual start times are determined. The *virtual start time adjustment* is shown in Figure 22b.

Table 21 – Time-shift factors for SMM test

Reference Stress (MPa)	ϕ_0	ϕ_1	ϕ_2	ϕ_3
290	1	0.59028	0.38342	0.22063

The *time-shift adjustment* (Step 4c) is performed by applying the self-calibration approach to the SSM data. The average creep strain rate (averaged over one hour) is found for the end of the reference stress level, σ_0 and beginning of the time-adjusted first stress level, σ_1 as shown in Figure 22c. The error between the two average creep strain rates is minimized numerically by

adjusting the C_1 and C_2 constants of WLF [Eq. (15)] until $\dot{\varepsilon}_{E,0} \cong \dot{\varepsilon}_{S,1}$ [Eq.(16)]. This process is repeated for every stress level. The ϕ values calculated for the SSM tests are provided in Table 21. After performing the self-calibration, the accelerated creep deformation and rupture curve is produced, as shown in Figure 22d. The SSM procedure performed in Figure 22 accelerated a 290 MPa creep test from 25.7 hr test to 52 hr with no discontinuity in creep strain information. All three creep regimes are easily identified in the accelerated creep curve.

The C_1 and C_2 constants of the WLF equation do not have appear to have a phenomenological significance in determining the time shift factor, C_2. This relationship can also be observed graphically.

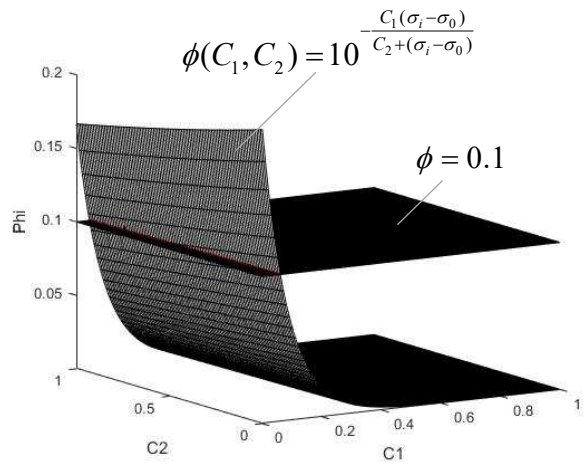

Figure 23 – Solutions to WLF equation for arbitrary values of $(\sigma_i - \sigma_0)$ and ϕ.

As shown in Figure 23, the values of C_1 and C_2 that satisfy $\phi = 0.1$ is the set of points that intersect the plane created by $\phi = 0.1$ and the surface created by the WLF equation. Therefore, there exist infinite combinations of non-zero C_1 and C_2 values that can produce a given time-shift factor.

Conclusion

In conclusion, a systematic approach to SSM has been developed for metallics and is applied to 304SS. The creep deformation and rupture accelerated with SSM agree well with data obtained from CCT. Therefore, SSM is a sound method for accelerating creep deformation and rupture at the stress and temperature levels investigated in this study. There are several considerations in applying the SSM procedure.

- The WLF equation [Eq. (15)] does not have a phenomenological significance for 304SS. It is shown that there are infinite non-zero values of the C_1 and C_2 material constants that satisfy the WLF equation for a given time-shift factor, ϕ_i. This indicates that the statistical dependence of C_1 and C_2 are negligible and ϕ_i can be found directly.
- The SSM procedure is a multi-step process prone to cumulative errors. For instance, specimen displacement is subject to fluctuations in thermal strain and extensometer slippage; erroneous strain measurements at this stage of SSM may accumulate when performing the systematic adjustments, thereby producing unrealistic results. The systematic approach outlined herein is designed to mitigate these issues.

Future Work

Future work should focus on assessing the limitations of SSM on metallics.

- A mechanistic equation that replaces the WLF equation should be developed. Ideally, the mechanistic equation should explain the physics of the time shift factor instead of being phenomenological.
- The number of stress levels, magnitude of stress steps, and duration of hold time may influence the shape of the accelerated creep curves or the distribution of the rupture life.

- The effect of temperature on the SSM procedure should be investigated.
- The effect of deformation mechanism transition on SSM should be experimentally proven.
- It should be investigated if SSM procedure can accelerate to extreme times (300,000 hr and beyond) by conducting SSM tests at low reference stresses.

References

[1] Viswanathan, R., and Foulds, J., 1998, "Accelerated Stress Rupture Testing for Creep Life Prediction – Its Value and Limitations," *Journal of Pressure Vessel Technology*, **120**(2), pp. 105-115.

[2] ASME, 2015, *ASME Boiler and Pressure Vessel Code, Section III, Division 1, Subsection NH – Class 1, Components in Elevated Temperature Service*, New York, NY.

[3] AFCEN, 2002, Règles de Conception et Construction – Mécanique Rapide (RCC-MR*)*, Design and Construction Rules for Mechanical Components of FBR Nuclear Islands AFCEN, Paris.

[4] EDF Energy, 2011, AGR Materials Data Handbook R66 Revision 9, Gloucester, UK.

[5] Ainsworth, R. A. (Ed.), 2003, *R5:* An Assessment Procedure for the High Temperature Response of Structures, Issue 3, British Energy Generation Ltd., Barnwood.

[6] Kim W., Park, J., Kim, S., Jang, J., 2013, "Reliability assessment of creep rupture life for Gr. 91 steel," *Materials and Design*, **51**, pp 1045-1051.

[7] Xing, L., Zhao, J., Shen, F., Feng W., 2006, "Reliability analysis and life prediction of HK40 steel during high-temperature exposure" *International Journal of Pressure Vessels and Piping*, **83**, pp 730-735.

[8] Zhao, J., Han, S., Gao, H., Wang, L., 2004, "Remaining life assessment of a CrMoV steel using the Z-parameter method," *International Journal of Pressure Vessels and Piping,* **81**, pp 757-760.

[9] Zhao, J., Li, D., Zhang, J., Feng, W, Fang, Y., 2009, "Introduction of SCRI model for creep rupture life assessment" *International Journal of Pressure Vessels and Piping*, **86**, pp 599-603.

[10] Choudhary, B.K., Kim, W., Mathew, M.D., Jang, J., Jayakumar, T., Jeong, Y., 2014, "On the reliability assessment of creep life for grade 91 steel," *Procedia Engineering*, **86**, pp 335-341.

[11] Solberg, J.K., 1982, "The influence of carbon and nitrogen on the high temperature creep properties of AISI type 316 austenitic stainless steel", *Materials Science and* Engineering, **55**, pp 39-44.

[12] Mathew, M.D., Sasikala, G., Rao, K., Mannan, S.L., 1991, "Influence of carbon and nitrogen on the creep properties of type 316 stainless steel at 873 K," *Materials Science and Engineering: A*, **148**(2), pp. 253-250.

[13] Sasikala, G., Mathew, M.D., Rao, K., Mannan, S.L., 1999, "Creep deformation and fracture behavior of a nitrogen-bearing type 316 stainless steel weld metal," *Journal of Nuclear Materials*, **273**, pp 257-264.

[14] Mathew, M.D., Laha, K., Ganesan, V., 2012, "Improving creep strength of 316 stainless steel by alloying with nitrogen," *Materials Science and Engineering A*, **535**, pp 76-83.

[15] Cottrell, A., 1995, An Introduction to Metallurgy, Second Edition, The Institute of Materials

[16] Yagi, K., 2008, “Acquisition of long-term creep data and knowledge for new applications,” *International Journal of Pressure Vessels and Piping*, **85**, pp 22-29.

[17] Holdsworth, S., 2008, “The European creep collaborative (ECCC) approach to creep data assessment,” *Journal of Pressure Vessel Technology*, **130**.

[18] Boyer, H.E., 1988, “Atlas of Creep and Stress-Rupture Curves,” *ASM International*.

[19] Simmons, W.F., Van Echo, J.A. 1965, “Report on the Elevated-Temperature Properties of Stainless Steels” *The ASTM-ASME Joint Committee on Effect of Temperature on the Properties of Metals ASTM Data Series Publication DS 5-S1”.*

[20] Smith, G.V., Heger, J.J., 1969, “Elevated Temperature Properties as Influenced by Nitrogen Additions to Types 304 and 316 Stainless Steels,” *ASTM Special Technical Publication 522*.

[21] Simmons, W.F., Cross, H.C. 1952, “Report on the Elevated-Temperature Properties of Stainless Steels,” *ASTM Special Technical Publication No. 124*.

[22] Xu, Y., Hosoya, J., Fujita A., Sakairi, Y., 2017, “Creep Data Sheet C6BJ” *National Institute for Materials Science, Materials Database Group.*

[23] Hill, M.R., 1976, “Mechanical Properties Test Data for Structural Materials,” Oakridge National Laboratories.

[24] Rohatgi, A., 2017, “WebPlotDigitizer,” *http://arohatgi.info/WebPlotDigitizer,* Accessed July 2017.

[25] Meyers, M.A., Chawla, K.K., 2009, “Mechanical behavior of materials,” Cambridge University Press.

[26] Mao, H., Mahadevan, S., 2000, “Reliability analysis of creep-fatigue failure,” *International Journal of Fatigue*, **22**, pp 789-797.

[27] Tummers, B., 2006, DataThief III. http://datathief.org/, Accessed September 12, 2016.

[28] Holdsworth, S.R., ECCC Recommendations Volume 5 Part Ia Issue 5, 2003.

[29] Higgins, R.A., 1993, Engineering Metallurgy Part I: Applied Physical Metallurgy, Sixth Edition, Arnold Press.

[30] Haque S.H. Ramirez, C., Stewart, C.M., 2017, Numerical Analysis of Time-Temperature Parameter Models Using Metamodeling, *Submitted to Journal of Pressure Vessel Technology.*

[31] F.R. Larson, J. Miller, 1952, *Transaction of ASME*, 74, pp. 765.

[32] Manson, S. S., and Haferd, A. M., 1953, “A Linear Time Temperature Relation for Extrapolation of Creep and Stress Rupture Data,” National Advisory Committee for Aeronautics.

[33] S.S. Manson, and W.F. Brown, 1953, *Proceedings of ASTM*, 53, pp. 683–719.

[34] R.L. Orr, O.D. Sherby, and J.E. Dorn, 1954, *Transaction of ASM*, 46, pp. 113–118.

[35] Manson, S. S., Succop, G., and Brown Jr, W. F., 1959, “The Application of Time-Temperature Parameters to Accelerated Creep-Rupture Testing,” *Transaction of ASM*, 51, pp. 911-934.

[36] Goldhoff, Robert M., and G. J. Hahn, 1968, "Correlation And Extrapolation Of Creep-Rupture Data Of Several Steels And Superalloys Using Time- Temperature Parameters".

[37] Spindler, S.L, Allen, D.J., Baker, A.J., and Spindler, M.W., 2010, Analysis of Cross-weld Creep Rupture Data on the ½Cr½Mo¼V Type IV Zone, International Journal of Pressure Vessels and Piping, Issue 87, pp. 296-303.

[38] Seruga, D., Fajdiga, M., and Nagode, M., 2011, Creep damage calculation for thermo-mechanical fatigue, Journal of Mechanical Engineering, Issue 57 Vol. 5, pp. 371-378.

[39] Haque, S. M., Ramirez, C., Stewart, C. M., 2017, “A Novel Metamodeling Approach for Time-Temperature Parameter Models”, *Proceedings of the ASME 2017 Pressure Vessels and Piping Conference*.

[40] Stewart, C. M., Chessa, J. F., 2016, “A Guideline for the Assessment of Uniaxial Creep and Creep-Fatigue Data and Models”, *DOE Funding Opportunity DE-FOA-0001488*.

[41] Engineering Properties of Steels, Philip D. Harvey, editor, American Society for Metals, Metals Park, OH, (1982).

[42] Handbook of Stainless Steels, Donald Peckner and I. M. Bernstein, McGraw-Hill Book Company, New York, NY, (1977)

[43] Metals Handbook, Howard E. Boyer and Timothy L. Gall, Eds., American Society for Metals, Materials Park, OH, 1985.

[44] Metals Handbook, 10th ed., vol. 1, ASM International Handbook Committee., ASM International, Materials Park, OH, (1990)

[45] United States Department of Energy, 2016, “Support of Fossil Energy Research and U.S. Colleges and Universities Including University Coal Research (UCR) and Research by Historically Black Colleges and Universities (HBC) and Other Minority Institutions (OMI),” DE-FOA-0001488.

[46] Stewart, C.M., 2008, “A hybrid constitutive model for creep, fatigue, and creep-fatigue damage,” Dissertation, University of Central Florida.

[47] National Science and Technology Council, “Advanced Manufacturing: A Snapshot of Priority Technology Areas Across the Federal Government,” Office of Science and Technology Policy, Washington, DC, 2016.

[48] U.S. Department of Energy Office of Science, “Basic Research Needs for Materials under Extreme Environments,” 2008. pp. 133

[49] Viswanathan, R., and Foulds, J., 1998, "Accelerated Stress Rupture Testing for Creep Life Prediction – Its Value and Limitations," *Journal of Pressure Vessel Technology*, **120**(2), pp. 105-115.

[50] ASME, 2015, *ASME Boiler and Pressure Vessel Code, Section III, Division 1, Subsection NH – Class 1, Components in Elevated Temperature Service*, New York, NY.

[51] AFCEN, 2002, *Règles de Conception et Construction – Mécanique Rapide (RCC-MR)*, Design and Construction Rules for Mechanical Components of FBR Nuclear Islands AFCEN, Paris.

[52] Ainsworth, R. A. (Ed.), 2003, *R5: An Assessment Procedure for the High Temperature Response of Structure*s, Issue 3, British Energy Generation Ltd., Barnwood.

[53] EDF Energy, 2011, AGR Materials Data Handbook R66 Revision 9, Gloucester, UK.

[54] Woodford, D. A. (1993). Test methods for accelerated development, design and life assessment of high-temperature materials. Materials & Design, 14(4), 231-242.

[55] Larson, F.R., Miller, J.A., Transactions ASME, "A Time-Temperature Relationship for Rupture and Creep Stresses", Vol. 74 pp. 765-771, 1952.

[56] R.L. Orr, O.D. Sherby, J.E. Dorn, Trans. ASM 46 (1956) 113–126.

[57] F.C. Monkman, N.J. Grant, Proc. ASM 56 (1956) 593.

[58] Ali, H.O., Tamin, M.N., Modified Monkman-Grant relationship for austenitic stainless steel foils. Journal of Nuclear Materials Vol 433, pp 74-79, 2013.

[59] Jazouli, S., Luo, W., Bremand, F., and Vu-Khanh, T., 2005, Application of time–stress equivalence to nonlinear creep of polycarbonate. *Polymer testing*, 24(4), 463-467.

[60] Luo, W. B., Wang, C. H., & Zhao, R. G., 2007, Application of time-temperature-stress superposition principle to nonlinear creep of poly (methyl methacrylate). In Key engineering materials (Vol. 340, pp. 1091-1096).

[61] Luo, W., Wang, C., Rongguo, Z. "Application of Time-Temperature-Stress Superposition Principle to Nonelinear Creep of Poly(methyl methcrylate)," Key Engineering Materials. Vols. 340-341, 2007, pp. 1091-1096.

[62] Giannopoulus, I.P., and Burgoyne C.J., 2009, "Stepped isostress method for aramid fibers" Proceedings of 8th International Conference on Fiber Reinforced Polymers for Reinforced Concrete Structures (FRPRCS9), Sydney, Australia.

[63] Giannopoulus, I.P., and Burgoyne C.J., 2009, "Stress limits for aramid fibres," Proceedings of the Institution of Civil Engineers – Structures and Buildings, 162(4), pp. 221-232.

[64] Burgoyne, C.J., 2011, "Allowable long term stresses in aramid yarns," First Middle East Conference on Smart Monitoring, Assessment, and Rehabilitation of Civil Structures, Dubai, UAE.

[65] Giannopoulos, I.P., and Burgoyne, C.J., 2011, “Prediction of the long-term behavior of high modulus fibers using SSM,” Journal of Materials Science, 46(24), pp. 7660-7671.

[66] Giannopoulos, I. P., and Burgoyne, C. J., 2012, “Accelerated and real-time creep and creep-rupture results for aramid fibers,” Journal of Applied Polymer Science, 125(5), pp. 3856-3870.

[67] Hadid, M., Guerira, B., Bahri, M., 2014, "Assessment of the stepped isostress method in the prediction of long term creep of thermoplastics," Polymer Testing, 34, pp. 113-119.

[68] M. Hadid, B. Guerira, M. Bahri & K. Zouani (2014) The creep master curve construction for the polyamide 6 by the stepped isostress method, Materials Research Innovations, 18(S6).

[69] Alabeweh F.S., Fogue M., Gbaguidi Aisse G.I., Talla P.K., “Stepped-iso-stress approach for bibolo: dibetou (lovoa trichilioides),” 1(5), pp. 255-269.

[70] Tanks, J.D., Rader, K., Sharp, S.R., 2015, “Accelerated creep testing of CFRP with the stepped isostress method,” Mechanics of Composite and Multi-functional Materials, Volume 7 Chapter 46, Springer International Publishing, Editor K. Zimmerman.

[71] Frost, H.J., and Ashby, M.F., (1982), “Deformation-Mechanism Maps, The Plasticity and Creep of Metals and Ceramics.” Pergamon Press, Oxford, England.

[72] Jazouli, S., Luo, W., Bremand, F., and Vu-Khanh, T. (2005). Application of time–stress equivalence to nonlinear creep of polycarbonate. *Polymer testing*, 24(4), 463-467.

[73] American Society of Testing and Methods, “ASTM Standard A276/A276M Specification for Stainless Steel Bars and Shapes,” ASTM International, West Conshohocken, PA, 2015.

[74] American Society of Testing and Methods, “ASTM Standard A479/A4796M Specification for Stainless Steel Bars and Shapes for Use in Boilers and Other Pressure Vessels,” ASTM International, West Conshohocken, PA, 2016.

[75] American Society of Testing and Methods, “ASTM Standard E8/E8M Test Methods for Tensions Testing of Metallic Materials,” ASTM International, West Conshohocken, PA, 2015.

[76] American Society of Testing and Methods, “ASTM Standard E139 Test Method for Conducting Creep, Creep-Rupture, and Stress-Rupture Tests of Metallic Materials,” ASTM International, West Conshohocken, PA, 2015.

[77] American Society of Testing and Methods, “ASTM Standard E21 Standard Test Methods for Elevated Temperature Tension Test of Metallic Materials,” ASTM International, West Conshohocken, PA, 2009.

[78] Talla, P.K., Alabeeh, F.S., Fogue, M., and Foadieng, E. “Time-stress equivalence applied to nonlinear creep of Bibolo: Diebtou (Lovoa trichilioides),” ARPN Journal of Engineering and Applied Sciences, Vol 9(1), 2014, pp. 50-60.

[79] Vincent, J., "Structural Biomaterials," Vol. 2016, Princeton University Press,

[80] Chevali, V.S., Dean, D.R., and Janowski, G.M., "Flexural creep behavior of discontinuous thermoplastic composites: Non-linear viscoelastic modeling and time–temperature–stress

superposition," Composites Part A: Applied Science and Manufacturing, Vol. 40, No. 6-7, 2009, pp. 870 877.

[81] Domis, 1973, "Creep and Creep-Rupture Properties of Types 304N and 316N Stainless Steels," ASTM Selected Technical Papers 522, American Society for Testing and Materials

[82] Simmons, W.F., and Van Echo, J.A., "Report on the Elevated-Temperature Properties of Stainless Steels," American Society of Testing and Materials, DS5S1, 1965.

[83] Kim, S. J., Kong, Y. S., Roh, Y. J., and Kim, W. G., 2008, “Statistical properties of creep rupture data distribution for STS304 stainless steels,” Materials Science and Engineering: A, 483, pp. 529-532.

Appendix

Flexible Analysis of Creep Database Matlab Code

```
function
[Model,StressParam,UniqueTemp,NumTemps,Data,NumData,RuptSim,RuptModel,ModelRa
w,ParamRaw,ParamSim,ModelCoeff,LogCoeff,...
    RuptRaw,R_Model,S_Temps,NMSE_Rupt,NMSE_Model,NMSE_Temps,RuptZS,RuptUTS] =
MetaModelvCR(Data,ModelName,StressParam)
% vCR03
% MetaModel Predict creep rupture using a time-temperature parameter model.
%   [RuptSim, ...] = MetaModel(D,M) returns creep rupture prediction (among
%   other variables), given the n-by-3 matrix D, using time-temperature
%   parameter model M. Creep rupture is predicted for each isotherm for the
%   stresses between 10 and 1000 MPa.
%
%   Columns 1, 2, and 3 of input D MUST correspond to temperature (C),
%   rupture time (hr), and stress (MPa).
%
%   Input M is a string containing the TTP model name. Valid model names
%   are provided in the full documentation.
%
%   By default, a logarithmic stress-parameter function is used to
%   parameterize the TTP of the form: TTP = z0 + z1*S + z2*log10(S), where:
%
%   z0, z1, z2 - coefficents
%   S          - stress (MPa)
%
% Examples
%   If Data = [600 14500 75; 600 15600 50; 700 12900 75; 700 9900 50];
%   and
%   Model = 'LM';
%   then
%   [RuptSim, ...] = MetaModel(Data,Model) will return creep rupture
%   predictions for isotherms 600C and 700C, using the Larson-Miller TTP.

%% Valid Model Names
% LM or LMP = Larson-Miller
% MH        = Manson-Haferd
% MB        = Manson-Brown
% OSD       = Orr-Sherby Dorn (not working)

%% Outputs
%%% RuptSim:    Predicted rupture for simulated values of stress.
%%% RuptModel:  Predicted rupture for actual values of stress.
%%% ModelRaw:   TTP values for raw data.
%%% ParamRaw:   Stress-parameter function evaluated for raw stress.
%%% ModelSim:   Stress-parameter function evaluated for simulated stress.
%%% ModelCoeff: Coefficients for the chosen TTP.
%%% LogCoeff:   Coefficients for the logarithmic stress-parameter function.
```

```
%%% R_Rupt:     Coeff. of determination (predicted vs. raw rupture times)
%%% R_Model:    Coeff. of determination (predicted vs. raw TTP values)
%%% R_Temps:    Coeff. of determination for each isotherm (predicted vs. raw
rupture times)
%%% NMSE_Rupt:  Normalized mean sq. error (all raw vs. predicted rupture)
%%% NMSE_Model: Normalized mean sq. error (all raw vs. predicted TTP values)
%%% NMSE_Temps: Normalized mean sq. error for each isotherm (predicted vs.
raw rupture times)

%% Constants
SimStress = logspace(0,3); % Simulated stress: 50 data points logarithmically
spaced from 10E0 to 10E3
SimData = [ones(length(SimStress),1), ones(length(SimStress),1), SimStress'];
% "Fake" data to simulate (temperature and rupture will be zeroed out; only
stress will be used)
NumData = length(Data);
Model = ModelName;

%% Metamodel Boundary Conditions
% Minimize error of the function "ModelObj" by changing unbounded values of
% "C", fitted to raw data points in "X". See Shafinul Haque's Metamodel
% manuscript for more details about the format of the metamodel.
%   ModelObj: (Metamodel) - (stress parameterization function)
%   RuptureFun: predicts rupture using the stress parameter function
%   (T: Temperature vector; P: TTP parameter vector; C: coefficient vector)
% Coefficient vector "C" corresponds to the metamodel coefficients:
%   [C(1), C(2), C(3), C(4), C(5), C(6), C(7), C(8), C(9), C(10)]
%   [a0,   a1,   a2,   r1,   r2,   q,    z0,   z1,   z2,   switch]
% Data matrix "X" corresponds to raw creep rupture data:
%   [X(:,1),      X(:,2),  X(:,3)]
%   [Temperature, Rupture, Stress]

%%% Metamodel Function
if strcmpi(ModelName,'CD') == 1 || strcmpi(ModelName,'MCD') == 1
    Meta = @(C,X) C(10).*( ((C(1).*X(:,3).^C(2)).*(X(:,1).^C(5))./((
X(:,1).^C(4) - C(3).^C(5) ).^C(6)) - log10(X(:,2))); % Metamodel by Md.
Shafinul Haque
else
    Meta = @(C,X) C(10).*(log10(X(:,2)) - C(1) -
C(2).*(X(:,1).^(C(5)))./(((X(:,1)).^C(4)-C(3).^C(5)).^C(6));
end

%%% Stress Parameter Function
if strcmpi(StressParam,'log') == 1
    SPF = @(C,X) -(C(7) + C(8).*X(:,3) + C(9).*log10(X(:,3))); % Stress
parameter function
elseif strcmpi(StressParam,'power') == 1
    SPF = @(C,X) -(C(7) + C(8).*X(:,3).^C(9));
```

```
elseif strcmpi(StressParam,'poly') == 1 || strcmpi(StressParam,'polynomial')
== 1
    SPF = @(C,X) -(C(7) + C(8).*X(:,3) + C(9).*X(:,3).^2);
elseif strcmpi(StressParam,'lin') == 1 || strcmpi(StressParam,'linear') == 1
    SPF = @(C,X) -(0.*C(7) + C(8) + C(9).*X(:,3));
elseif strcmpi(StressParam,'exp') == 1 || strcmpi(StressParam,'Exponential')
== 1
    SPF = @(C,X) -(C(7) + C(8).* exp(C(9).*X(:,3)));
else
    error('Invalid stress parameter function. View documentation for valid
functions.')
end

%%% Objective Function
ModelObj = @(C,X) (Meta(C,X) + SPF(C,X));

% Upper and lower bounds format: [a0, a1, a2, r1, r2, q, z0, z1, z2, switch]
if strcmpi(ModelName,'LM') == 1 || strcmpi(ModelName,'LMP') == 1
%        [a0,   a1, a2,  r1,  r2, q,     z0,    z1,    z2, switch]
    ub = [Inf,   0,  0,   -1,  1,  1,   Inf,     1e5,   Inf,  1]; % upper
bounds
    lb = [-Inf,   0,  0,   -1,  1,  1,  -Inf,    -Inf,   -Inf,  1]; % lower
bounds
    x0 = [-19,    0,  0,   -1,  1,  1,    0,   31768,    -0.096,  1]; %
initial guess
    RuptureFun = @(T,P,C) 10.^(P./(T)+C(1)); % Rupture time as a function of
TTP

elseif strcmpi(ModelName,'MH') == 1
%        [a0,     a1, a2, r1, r2, q, z0, z1, z2, switch]
%        [log(ta), 0, Ta, 1,  1,  1, z0, z1, z2, switch]
    ub = [Inf,  0,  Inf, 1, 1, 1, Inf,   Inf,  Inf, 1]; % upper bounds
    lb = [-Inf, 0, -Inf, 1, 1, 1, -Inf, -Inf, -Inf, 1]; % lower bounds
    x0 = [20,   0,  0,   1 ,1, 1, 1E4,   1,   -1E3, 1]; % initial guess
    RuptureFun = @(T,P,C) 10.^(P.*(T-C(3))+C(1));

elseif strcmpi(ModelName,'MB') == 1
%        [a0,      a1,   a2,  r1, r2,  q,    z0,    z1,   z2,  switch]
%        [log(ta), 0,    Ta,  1,  1,   n,    z0,    z1,   z2,  switch]
    ub = [Inf,     0,   Inf,  1,  1,   Inf,   Inf,   Inf,   Inf,   1]; %
upper bounds
    lb = [-Inf,    0,  -Inf,  1,  1,   -Inf, -Inf,  -Inf,   -Inf,  1]; %
lower bounds
    x0 = [14,     0,    25,   1,  1,   2,    -2E-5,  -2E-7, 3E-10, 1]; %
initial guess
    RuptureFun = @(T,P,C) 10.^(P.*(T-C(3)).^C(6)+C(1));

elseif strcmpi(ModelName,'OSD') == 1
%        [a0, a1,  a2,   r1,  r2, q, z0, z1, z2, switch]
```

```
%        [0,  Q/R, 1,    1,   -1, 0, z0, z1, z2, switch]
    ub = [0,  Inf,  1,  1,  -1,  0,  Inf,   Inf,  Inf, 1]; % upper bounds
    lb = [0, -Inf,  1, 1,  -1,  0, -Inf,  -Inf, -Inf, 1]; % lower bounds
    x0 = [0,  1E5,  1,    1,  -1,  0,  1E4,   1,   -1E3, 1]; % initial guess
    RuptureFun = @(T,P,C) 10.^(P+C(2)./(T));

elseif strcmpi(ModelName,'MS') == 1
%        [a0, a1,  a2, r1, r2,  q,  z0,   z1,  z2,    switch]
%        [0,  Q/R, 1,  1,  -1,  0,  z0,   z1,  z2,    switch]
    ub = [0,  Inf, 0,  1,   1,  0,  Inf,  Inf,  Inf,    1]; % upper bounds
    lb = [0, -Inf, 0,  1,   1,  0, -Inf, -Inf, -Inf,    1]; % lower bounds
    x0 = [0,  1E4, 0,  1,   1,  0,  1E4,   0,  40,   -.1]; % initial guess
    RuptureFun = @(T,P,C) 10.^(P+C(2).*(T));

elseif strcmpi(ModelName,'GW') == 1
%        [a0, a1,   a2,  r1, r2,   q,  z0,    z1,   z2,    switch]
%        [0,  Q/R,  1,   1,  -1,   0,  z0,    z1,   z2,    switch]
    ub = [0,   0,  Inf,  1,   1,   3,  Inf,  Inf,  Inf,    1]; % upper bounds
    lb = [0,   0,  -Inf, 1,   1,   3, -Inf, -Inf, -Inf,    1]; % lower bounds
    x0 = [0,   0,  1005,  1,   1,   3,  -1E-7,   0,  1E-3,    1]; % initial
guess
    RuptureFun = @(T,P,C) 10.^(P.*(((T)-C(3)).^C(6)));

elseif strcmpi(ModelName,'CD') == 1
%        [a0,     a1,  a2, r1, r2,  q,  z0,   z1,  z2,    switch]
%        [a,      b,   1,  1,   1,  0,  z0,   z1,  z2,    switch]
    ub = [Inf,   Inf,   1, 1,   1,  0,  Inf,  Inf,  Inf,   1]; % upper bounds
    lb = [-Inf,  -Inf,  1, 1,   1,  0, -Inf, -Inf, -Inf,   1]; % lower bounds
    x0 = [1e3,   1,     1, 1,   1,  0,   1E3,  1.4,  0.6, 1]; % initial guess
    RuptureFun = @(T,P,C,S) 10.^((C(1).*S.^C(2)).*T-P);
%(C(1).*X(:,3).^C(2))

elseif strcmpi(ModelName,'GS') == 1
%        [a0,   a1,   a2,   r1,  r2,   q,   z0,   z1,  z2,    switch]
%        [0,    Q/R,  1,    1,   -1,   0,   z0,   z1,  z2,    switch]
    ub = [Inf,   0,   Inf,  -1,   -1,   1,  Inf,  Inf,  Inf,    1]; % upper
bounds
    lb = [-Inf,  0,   -Inf, -1,   -1,   1, -Inf, -Inf, -Inf,    1]; % lower
bounds
    x0 = [32,    0,   248,  -1,   -1,   1,  1E4,   27,  -.05,    1]; %
initial guess
    RuptureFun = @(T,P,C) 10.^(P.*((T).^-1-C(3).^-1)+C(1));

elseif strcmpi(ModelName,'MMH') == 1
%        [a0,   a1,  a2, r1, r2,  q,  z0,   z1,  z2,    switch]
%        [0,    Q/R, 1,  1,  -1,  0,  z0,   z1,  z2,    switch]
    ub = [Inf,   0,  0,  1,   1,  1,  Inf,  Inf,  Inf,    1]; % upper bounds
    lb = [-Inf,  0,  0,  1,   1,  1, -Inf, -Inf, -Inf,    1]; % lower bounds
    x0 = [25,    0,  0,  1,   1,  1,  1E4,   1,  -1E3,   1]; % initial guess
```

```
    RuptureFun = @(T,P,C) 10.^(P.*(T)+C(1));

elseif strcmpi(ModelName,'MGW') == 1
%        [a0, a1,   a2,  r1,  r2,   q,   z0,   z1,    z2,    switch]
%        [0,  Q/R,  1,   1,   -1,   0,   z0,   z1,    z2,    switch]
    ub = [0,   0,  Inf,  -1,  -1,    2,  Inf,  Inf,   Inf,    1]; % upper
bounds
    lb = [0,   0, -Inf,  -1,  -1,    2, -Inf, -Inf, -Inf,    1]; % lower
bounds
    x0 = [0,   0,  900,   -1,  -1,   2,    1E4,   7E8,   -0.975,   1]; %
initial guess
    RuptureFun = @(T,P,C) 10.^(P.*(((T).^-1-C(3).^-1).^C(6)));

elseif strcmpi(ModelName,'MCD') == 1
%        [a0,    a1,  a2, r1, r2, q,  z0,   z1,  z2,    switch]
%        [a,     b,   1,  -1, -1,  0,  z0,   z1,  z2,    switch]
    ub = [Inf,   Inf, 1,  -1,  -1,  0,  Inf,  Inf,  Inf,   1]; % upper bounds
    lb = [-Inf, -Inf, 1,  -1,  -1,  0, -Inf, -Inf, -Inf,   1]; % lower bounds
    x0 = [1e3,   1,   1,  -1   -1,  0,  1E4,   1,  -1E3,   1]; % initial
guess
    RuptureFun = @(T,P,S,C) 10.^((C(1).*S.^C(2))./T-P);
%(C(1).*X(:,3).^C(2))

elseif strcmpi(ModelName,'MGS') == 1
%        [a0,   a1,  a2,     r1, r2,   q,  z0,   z1,  z2,    switch]
%        [0,    Q/R, 1,      1,  -1,   0,  z0,   z1,  z2,    switch]
    ub = [Inf,   0,  Inf,   -1,  -1,   2,  Inf,  Inf,  Inf,    1]; % upper
bounds
    lb = [-Inf,  0,  -Inf,  -1,  -1,   2, -Inf, -Inf, -Inf,    1]; % lower
bounds
    x0 = [520,    0,  12.4, -1,  -1,   2,  -1E5,   -15,  0.31,   1]; %
initial guess
    RuptureFun = @(T,P,C) 10.^(P.*(((T).^-1-C(3).^-1).^C(6))+C(1));

elseif strcmpi(ModelName,'Wild') == 1
%        [a0,   a1,   a2,     r1, r2,   q,  z0,   z1,  z2,    switch]
%        [0,    Q/R,  1,      1,  -1,   0,  z0,   z1,  z2,    switch]
    ub = [Inf,   Inf,  Inf,   -1, -1,   1,  Inf,  Inf,  Inf,    1]; % upper
bounds
    lb = [-Inf,  -Inf, -Inf,  -1,  -1,   1, -Inf, -Inf, -Inf,    1]; % lower
bounds
    x0 = [20,     700,   25,     -1,  -1,   1,  .01,   1.1E4,  20,    1]; %
initial guess
    RuptureFun = @(T,P,C) 10.^(P.*(((T).^C(4)-
C(3).^C(5)).^C(6))+C(1)+C(2).*(T).^C(5));

    %C(10).*(log10(X(:,2)) - C(1) -
C(2).*(X(:,1).^(C(5))))./(((X(:,1)).^C(4)-C(3).^C(5)).^C(6))
```

```
else
    error('Invalid model name. View documentation for valid model names.')
end

%% Model Optimization and Constants
Coeff  = lsqnonlin(@(C)ModelObj(C,Data),x0,lb,ub); % Minimize error and write
coefficients to "Coeff"

ModelCoeff = [1,1,1,1,1,1,0,0,0,1].*Coeff; % Model coeff's (zeros out coeff's
for stress parameter function)
LogCoeff   = [0,0,0,0,0,0,1,1,1,0].*Coeff; % Stress parameter function
coeff's (zeros out coeff's for TTP model)

ModelRaw = ModelObj(ModelCoeff,Data);    % TTP model evaluated at raw data
points
ParamRaw = -ModelObj(LogCoeff,Data);     % Stress-parameter function
evaluated at raw stress
ParamSim = -ModelObj(LogCoeff,SimData);  % Stress-parameter function
evaluated at simulated stress

%% UTS Calculation
% UTS = 580;
% IsoUTS = [550;600;650;700;750;800;850];

UTS = [580;430;83]; % corresponds to IsoUTS below
IsoUTS = [25;450;920]; % corresponds to UTS above
X = ones(numel(UTS),1);
Y = ones(numel(UTS),1);
FakeUTS = [IsoUTS,Y,UTS];
RuptUTS = zeros(numel(IsoUTS),1);
% ParamUTS = zeros(numel(IsoUTS),1);
ParamUTS = -ModelObj(LogCoeff,FakeUTS);

for n = 1:numel(IsoUTS);
    RuptUTS(n) = RuptureFun(IsoUTS(n),ParamUTS(n),ModelCoeff);
end
RuptUTS = RuptUTS';
%% Zero Stress Calculation
ZS = 10E-10;
IsoUTS = [550;600;650;700;750;800;850];
ParamZS = -ModelObj(LogCoeff,[1,1,ZS]);
for n = 1:numel(IsoUTS);
    RuptZS(n) = RuptureFun(IsoUTS(n),ParamZS,ModelCoeff);
end

%% Rupture Predictions
%%% Temperature sorting
UniqueTemp  = unique(Data(:,1));  % Unique temperatures
NumTemps    = length(UniqueTemp); % Number of unique temperatures
```

```
RuptSim     = cell(NumTemps,1);   % Predicted rupture times, for values of
SimStress
RuptModel   = cell(NumTemps,1);   % Predicted rupture times, for values of
RawStress
RuptRaw     = cell(NumTemps,1);   % Raw rupture times sorted to match order
of RuptModel
S_Temps     = zeros(NumTemps,1);  % Coeff. of determination for each isotherm
NMSE_Temps  = zeros(NumTemps,1);  % NMSE for each isotherm

%%% Evaluate for each isotherm
for n = 1:NumTemps
    TempIdx       = (Data(:,1) == UniqueTemp(n)); % Logical indices of each
unique temperature
    RuptRaw{n}    = Data(TempIdx,2);              % Raw rupture

    if strcmpi(ModelName,'CD') ==1 || strcmpi(ModelName,'MCD') == 1
        RuptSim{n}    =
RuptureFun(UniqueTemp(n),ParamSim,SimStress,ModelCoeff);
        RuptModel{n}  =
RuptureFun(UniqueTemp(n),ParamRaw(TempIdx),Data(TempIdx,3),ModelCoeff);
    else
        RuptSim{n}    = RuptureFun(UniqueTemp(n),ParamSim,ModelCoeff);
% Rupture evaluated for simulated stress
        RuptModel{n}  =
RuptureFun(UniqueTemp(n),ParamRaw(TempIdx),ModelCoeff); % Rupture evaluated
for raw stress
    end

    S_Temps(n)    = std(RuptRaw{n});                      % Coeff. of
determination for each isotherm (raw vs. predicted rupture)
    NMSE_Temps(n) = NMSE(RuptRaw{n},RuptModel{n});                          %
NMSE of each isotherm (raw vs. predicted rupture)
end

%% Residuals and Coefficient of Determination (R-Squared)
R_Model = RSquared(ModelRaw,ParamRaw);                          % R-Squared
for the TTP model
R_Rupt  = RSquared(vertcat(RuptRaw{:}),vertcat(RuptModel{:})); % R-squared
for predcited rupture times

%% Normalized Mean Square Error (NMSE)
NMSE_Model = NMSE(ModelRaw,ParamRaw);                          % NMSE for the
TTP model (stress paprameter function)
NMSE_Rupt  = NMSE(vertcat(RuptRaw{:}),vertcat(RuptModel{:})); % NMSE for
predicted rupture
```

Stepped Isostress Method Matlab Code

```
%% SSM BEGIN

%% Create directories and filename.

%%% IMPORTANT! To run this m-file, you must change 'dir' to the directory
%%% where the raw files are located on your computer.

%dir = 'E:\Instron Tests\Stepped Isostress\SSM-2\SSM-2.is_tcyclic_RawData\';
dir = 'C:\Users\Chris\Google Drive\UTEP\MERG\Accelerated Creep\Tensile
Tests\SSM-2\SSM-2.is_tcyclic_RawData\';
csv = 'Specimen_RawData_1.csv'; % Raw filename for all tests.

file = [dir csv];

%% Raw data columns are:
% |     1    |      2         |     3    |          4           |         5
|          6             |       7         |
% | Time (s) | Extension (in) | Load (N) | Tensile Stress (MPa) | Tensil
Extension (in) | Tensile Strain (in/in) | Epsilon (in/in) |

%% Import Files

fid = fopen(file,'rt');
ssmheaders = textscan(fid,'%s',7,'delimiter',','); % There are seven data
columns.
ssmraw =
textscan(fid,(repmat('%f',[1,7])),'delimiter',',"','CollectOutput',1,'headerl
ines',2,'MultipleDelimsAsOne',true);
fclose(fid);
% The 'ssmrawdata' variables are cells nested within a cell. The loop below
% will extract them so there is no nested cell nonsense going on.

temp = cell(1,7);
for i = 1:7
   temp{i} = ssmraw{1}(:,i);
end
ssmraw = temp;

%% Truncate data so that all start at zero.
    % Find first value of appreciable tensile stress. In this case, 0.75
    % MPa is arbitrarily chosen. This section of code will throw out the
    % data acquired during the preload sequence, which is not relevant.
    % NOTE: The 'SSM' matrix below will contain all the relevant test
    % values. The data type in each column of 'SSM' are the same as the
    % columns in 'rawdata' above.
```

```
index = find(ssmraw{4} > 0.75, 1); % Search tensile stress (column 4) for the
first value greater than 0.75 MPa.
L = length(ssmraw{4}(index:end)); % Length of relevant data.

SSM = cell(1,7);
for i = 1:7,
    SSM{i} = ssmraw{i}(index:end); % Populate SSM cell array.
end

%% Plot Raw Data

% timeraw = (ssmraw{1}/3600);
% epsilonraw = ssmraw{7};
% stressraw = ssmraw{4};
%
% %
% figure
% [ax a1 a2] = plotyy(timeraw,epsilonraw,timeraw,stressraw);
% title('Strain vs. Time (Specimen 2 full range)')
% xlabel('Time (hours)'), ylabel('Strain (in/in)')
% axes(ax(2)); ylabel('Stress MPa');
% grid on

%% Define data vectors.

time = SSM{1}/3600; % Time in seconds
stress = SSM{4}; % Stress
xtn = SSM{5}; % Extension, Instron crosshead
strain = SSM{6}; % Strain, Instron crosshead
epsilon = SSM{7}; % Epsilon extensometer strain

%% Horizontal Offset for Strain
    % Make strain, stress, and time start at zero on x-axis.
ssorg = stress;
eeorg = epsilon;
ttorg = time;

strain = strain - strain(1); % Strain from crosshead
epsilon = epsilon - epsilon(1); % Strain from extensometer
xtn = xtn - xtn(1); %Tensile extension
    xtn1 = 1 + xtn; % Create strain vector from extension information. Define
'xtn1' as "original" length of 1.
    engstrain = (xtn1./1 -1); % strain = (instantaneous length/original
length - 1)
time = time - time(1); % Time.
    time = time; % Convert seconds to hours.
    ramptime = 1/60; % Each ramp lasted 1 minute, or 1/60th of an hour.

%% Adjustments
```

```
%%% Unmodified
    %%% Make no adjustments to the data except remove ramps at beginning
    %%% and end of test.

% Make copy of data to work on it.
ee = epsilon; tt = time; ss = stress; xx = engstrain;

% Remove ramp down after test ended.
ee(721620:end) = [ ];
tt(721620:end) = [ ];
ss(721620:end) = [ ];

% Remove ramp up just after test began.
ee(1:743) = [ ];
tt(1:743) = [ ];
ss(1:743) = [ ];

%%% Unmodified Stress & Creep vs. Time.
% subplot(1,2,1)
% [ax, a1, a2] = plotyy(tt,ee,tt,ss); % Plot strain from extensometer.
% set([a1;a2],'LineStyle','none','Marker','.')
% title('Creep & Stress vs. Time (area of interest)')
% xlabel('Time (Hours)'); ylabel('Creep Strain(in/in)')
% xlim([0 20])
% axes(ax(2)); ylabel('Stress (MPa)');
% xlim([0 20])
% grid on
%%
%%% Fictitious Drops
    % Custom function: shrink(xx, start, end). The data between
    % 'start' and 'end' of vector 'xx' will be deleted and joined to make a
    % continuous curve.
    % NOTE: All indeces are chosen by visually examining the graphs.
    % NOTE: Do not shrink stress, otherwise the stress levels are lost and
    % the stress-time plot shows a flat line.

% Copy data to work on it.
ee = epsilon; tt = time; ss = stress; xx = engstrain;

% Remove fictitious drop in region 1.
ee = shrink(ee,49857,50014);
tt = shrink(tt,49857,50014);
ss(49857:50014) = [ ];
xx = shrink(xx,49857,50014);

% Remove fictitious drop in region 3.
ee = shrink(ee,486863,497367);
tt = shrink(tt,486863,497367);
```

```
ss(486863:497367) = [ ];
xx = shrink(xx,486863,497367);

% Remove cool down ramp after region 4.
ee(711748:end) = [ ];
tt(711748:end) = [ ];
ss(711748:end) = [ ];
xx(711748:end) = [ ];

% Remove ramp up before region 1.
cut = 743;
ee(1:cut) = [ ];
tt(1:cut) = [ ];
ss(1:cut) = [ ];
xx(1:cut) = [ ];

del = cut - 604;
% Originally used 1:604, now using 1:cut. All values below must now be
% shifted by the difference between new and old (del).
% If need to keep elastic strain for McVetty fit, use 492.

%%% Adjustments #1 & 2: Initial & Vertical Shifting (remove ramps).
    % Ramps should be removed last to first; otherwise, the hand-selected
    % indeces below will not match.

% Ramp from region 3 to region 4.
ee = shrink(ee,530547-del,531171-del);
tt = shrink(tt,530547-del,531171-del);
xx = shrink(xx,530547-del,531171-del);
ss(530547-del:531171-del) = [ ];

% Ramp from region 2 to region 3.
ee = shrink(ee,360437-del,361059-del);
tt = shrink(tt,360437-del,361059-del);
xx = shrink(xx,360437-del,361059-del);
ss(360437-del:361059-del) = [ ];

% Ramp from region 1 to region 2.
ee = shrink(ee,179832-del,180501-del);
tt = shrink(tt,179832-del,180501-del);
xx = shrink(xx,179832-del,180501-del);
ss(179832-del:180501-del) = [ ];

%%% Modified Stress & Creep vs. Time.
% subplot(1,2,2)
% [ax, a1, a2] = plotyy(tt,ss,tt,ee); % Plot strain from extensometer.
% set([a1;a2],'LineStyle','none','Marker','.','LineWidth',4)
% title('Creep & Stress vs. Time','FontSize',20) %(Adjustments 1 & 2)
% xlabel('Time (Hours)'); ylabel('Stress (MPa)');
```

```
% axes(ax(2)); ylabel('Creep Strain(in/in)');
% grid on

%% Adjustment #3: Rescaling
    % Fit each region to a polynomial to find its x-intercept.
    % Shift each curve to zero based on its respective x-intercept.

% Define Regions
tcell = cell(1,4);
rcell = cell(1,4);

tcell{1} = tt(1:179831-del); % Originally using 400:179831, but why?
rcell{1} = ee(1:179831-del); % Originally using 400:179831, but why?

tcell{2} = tt(179832-del:359766-del);
rcell{2} = ee(179832-del:359766-del);

tcell{3} = tt(359767-del:529253-del);
rcell{3} = ee(359767-del:529253-del);

tcell{4} = tt(529254-del:end);
rcell{4} = ee(529254-del:end);

rcellcopy = rcell;
offset = rcell{1}(1); % Make creep start at zero to get correct intercepts.
for i = 1:4
   rcell{i} = rcell{i} - offset;
end

%% McVetty Model Fit
% Time data (tcell) and strain data (rcell).
% Shift all values to zero strain and zero time. Otherwise, McVetty doesn't
% fit well.
% McVetty = G*(1-exp(-q*t))+H*t
% 'MVcoeff' order is: [G, H, q]
% Adustment # 3 - Rescaling.
% 1. Find McVetty model fit for each stress level. McVetty works best if it
% starts from zero, so all strain data is shifted to zero strain and zero
% time.
% 2. Find virtual start time (point where McVetty crosses the x-axis).

MVx1 = tcell{1};
MVy1 = rcell{1};

MVx2 = tcell{2} - tcell{2}(1); % Shift to zero time.
MVy2 = rcell{2} - rcell{2}(1); % Shift to zero strain.

MVx3 = tcell{3} - tcell{3}(1);
MVy3 = rcell{3} - rcell{3}(1);
```

```
MVx4 = tcell{4} - tcell{4}(1);
MVy4 = rcell{4} - rcell{4}(1);

[MVfitresults, MVgof] = McVetty_fit(MVx1, MVy1, MVx2, MVy2, MVx3, MVy3, MVx4,
MVy4);

MVcoeff = cell(1,4);
for i = 1:4
   MVcoeff{i} = coeffvalues(MVfitresults{i});
end

%% Adj. #3 - Linear Rescale
% Using McVetty primary creep model to find virtual start times for each
% stress level.

t = linspace(-10,20); % Large enough interval to accomodate all stress
levels.
enot = [0, rcell{2}(1), rcell{3}(1), rcell{4}(1)];

MV_y = cell(1,4);
MV_poz = cell(1,4);
t_off = zeros(1,4);
MV_int = zeros(1,4);
idx = zeros(1,4);
tlin = cell(1,4); % Linearly rescaled time.

for i = 1:4
    G = MVcoeff{i}(1);
    H = MVcoeff{i}(2);
    q = MVcoeff{i}(3);

    MV_y{i} = G*(1-exp(-q.*t))+H.*t + enot(i);
    MV_poz{i} = abs(MV_y{i});

    idx(i) = find(abs(MV_y{i}) == min(abs(MV_poz{i})));
    t_off(i) = abs(t(idx(i)));
    MV_int(i) = tcell{i}(1) - t_off(i);
    tlin{i} = tcell{i} - MV_int(i);
end
elin = rcell; % Rename strain cell array because what the eff is rcell?!

%%
% Plot McVetty fit vs. actual data.

%%% Build polynomial array holding coefficients.
x = linspace(0,20);
p = cell(3,4); % Array to hold polynomial coefficients.
sim = cell(3,4); % Array to hold y-data for fitted lines.
```

```
xint = zeros(4,4); %Define empty x-intercept matrix to fill out.
tsim = cell(1,4); % Define empty cells for fitted time for each region.

for i = 1:3; % polynomial order
    for j = 1:4; % stress region
        p{i,j} = polyfit(tcell{j},rcell{j},i); % Populate array with
polynomial coefficients.
        sim{i,j} = polyval(p{i,j},x);
        xint(i,j) = min(roots(p{i,j}));
        tsim{i,j} = tcell{j} - xint(i,j);
    end
end

% Modify first region so there is no x-intercept adjustment.
tsim{1,1} = tsim{1,1} + xint(1,1);
% Modify x-intercept for first region based on McVitty model.
% xint(4,1) = real(min(roots(model)));

%% Adjustment # 4 Horizontal shifting

ref = [245.72; 249.68; 253.65; 257.61]; %Stresses for each stress level in
MPa
J = cell(1,4); % Creep compliance.
T = cell(4,4); % Shifted time.
A = zeros(1,4); % Stress shift factor.

% Constants
C1 = 1;
C2 = 2;
a = [0.1, 0.1, 0.1, 0.1]; %shift factor, guess values
for i = 1:4
    A(i) = 10^(-(C1*(ref(i)-ref(1)))/(C2+(ref(i)-ref(1)))); %shift factor
based on C1, C2.
end

% Creep compliance is strain divided by constant stress level.
for i = 1:4,
    J{i} = rcell{i}./ref(i); % Strain for a given stress level (i) divided by
its stress level.
    T{1,i} = tsim{1,i}./a(i); % Reduced time, linear rescale time, based on
guess values of a.
    T{2,i} = tsim{1,i}./A(i); % Reduced time based on guess values of C1, C2.
    T{3,i} = tcell{i}; % Reduced time, original time.
end

ratio = [1, ref(2)/ref(1), ref(3)/ref(1), ref(4)/ ref(1)];

%% Plots %%
%%%%%%%%%%
```

```
%%%%%%%%%%
%% SSM-2, Adjustment #2
% Vertical adjustment and comparison of vertical adjustment.

figure
subplot(1,2,1)
for i = 1:4
    plot(tcell{i},rcell{i})
    hold on
end
    hold off
title('SSM-2, After Vertical Adjustment & Offset')
xlabel('Time (hours)'), ylabel('Strain in/in');
legend('62% YS','63% YS','64% YS','65% YS','Location','southeast')
ylim([0 0.04])
grid on

subplot(1,2,2)
for i = 1:4
    plot(tcell{i},rcellcopy{i})
    hold on
end
    hold off
title('SSM-2, After Vertical Adjustment, No Offset')
xlabel('Time (hours)'), ylabel('Strain in/in');
legend('62% YS','63% YS','64% YS','65% YS','Location','southeast')
ylim([0 0.04])
grid on

%%

SSM1 = [tcell{1} rcell{1}];
SSM2 = [tcell{2} rcell{2}];
SSM3 = [tcell{3} rcell{3}];
SSM4 = [tcell{4} rcell{4}];
%
% csvwrite('SSM1.csv',SSM1);
% csvwrite('SSM2.csv',SSM2);
% csvwrite('SSM3.csv',SSM3);
% csvwrite('SSM4.csv',SSM4);

%% Linear rescale, all stress levels
figure
    plot(tsim{1,1},rcell{1},'r.')
        hold on
    plot(tsim{1,2},rcell{2},'g.')
    plot(tsim{1,3},rcell{3},'b.')
    plot(tsim{1,4},rcell{4},'k.')
        hold off
```

```
    title('Creep Strain vs. Time (Linear Rescale)');
    xlabel('Time (Hours)'); ylabel('Creep Strain (in/in)')
    grid on

%% Fitted Data
    % Linear plots
    figure
    subplot(3,2,1)
    hold on
    plot(tcell{1},rcell{1},'r.',x,sim{1,1},'r')
    plot(tcell{2},rcell{2},'g.',x,sim{1,2},'g')
    plot(tcell{3},rcell{3},'b.',x,sim{1,3},'b')
    plot(tcell{4},rcell{4},'k.',x,sim{1,4},'k')
    title('Creep Strain vs. Time (Linear Fit)');
    xlabel('Time (Hours)'); ylabel('Creep Strain (in/in)')
    xlim([-40 20])
    ylim([0 0.04]);

    % Second-order plot.
    subplot(3,2,3)
    hold on
    plot(tcell{1},rcell{1},'r.',x,sim{2,1},'r')
    plot(tcell{2},rcell{2},'g.',x,sim{2,2},'g')
    plot(tcell{3},rcell{3},'b.',x,sim{2,3},'b')
    plot(tcell{4},rcell{4},'k.',x,sim{2,4},'k')
    title('Creep Strain vs. Time (2^{nd} Order Fit)');
    xlabel('Time (Hours)'); ylabel('Creep Strain (in/in)')
    xlim([-20 20]);
    ylim([0 0.04]);

    % Third order plot.
    subplot(3,2,5)
    hold on
    plot(tcell{1},rcell{1},'r.',x,sim{3,1},'r')
    plot(tcell{2},rcell{2},'g.',x,sim{3,2},'g')
    plot(tcell{3},rcell{3},'b.',x,sim{3,3},'b')
    plot(tcell{4},rcell{4},'k.',x,sim{3,4},'k')
    title('Creep Strain vs. Time (3^{rd} Order Fit)');
    xlabel('Time (Hours)'); ylabel('Creep Strain (in/in)')
    ylim([0 0.04]);

%%% Linear
    subplot(3,2,2)
    plot(tsim{1,1},rcell{1},'r.')
        hold on
    plot(tsim{1,2},rcell{2},'g.')
    plot(tsim{1,3},rcell{3},'b.')
    plot(tsim{1,4},rcell{4},'k.')
        hold off
```

```
    title('Creep Strain vs. Time (Linear Rescale)');
    xlabel('Time (Hours)'); ylabel('Creep Strain (in/in)')
    grid on
    ylim([0 0.04]);
%axis([0 60 0.015 0.04])

%%% Second-order rescale
    subplot(3,2,4)
    hold on
    plot(tsim{2,1},rcell{1},'r.')
    plot(tsim{2,2},rcell{2},'g.')
    plot(tsim{2,3},rcell{3},'b.')
    plot(tsim{2,4},rcell{4},'k.')
    title('Creep Strain vs. Time (2^{nd} Order Rescale)');
    xlabel('Time (Hours)'); ylabel('Creep Strain (in/in)');
    grid on
    ylim([0 0.04]);
%axis([0 60 0.015 0.04])

%%% Third-order rescale
    subplot(3,2,6)
    hold on
    plot(tsim{3,1},rcell{1},'r.')
    plot(tsim{3,2},rcell{2},'g.')
    plot(tsim{3,3},rcell{3},'b.')
    plot(tsim{3,4},rcell{4},'k.')
    title('Creep Strain vs. Time (3^{rd} Order Rescale)');
    xlabel('Time (Hours)'); ylabel('Creep Strain (in/in)');
    [h,icons,plots,str] = legend('Stress 1 (62% YS)','Stress 2 (63%
YS)','Stress 3 (64% YS)','Stress 4 (65%
YS)','Location','southeast','Orientation','horizontal');
    set(h,'FontSize',12);
    set(icons(:),'LineStyle','-','LineWidth',2); %// Or whatever
    grid on
    ylim([0 0.04]);
%axis([0 60 0.015 0.04])


%% McVetty Model
% Each stress level modeled, but shifted to time = zero.
hold on
for i = 1:4
    plot(t,MV_y{i}+enot(i))
end
hold off
grid on
title('McVetty Models (time shifted to zero)')
xlabel('Time (hours)'), ylabel('Strain (in/in)')
legend('Stress 1','Stress 2','Stress 3','Stress 4','Location','southeast')
```

```
ylim([0  0.03])
%% McVetty Model
% Linear rescale; next step is horizontal shift
figure
hold on
for i = 1:4
   plot(tlin{i},elin{i})
end
hold off
title('Linearly Rescaled (McVetty)')
xlabel('Time (hours)'), ylabel('Strain (in/in)');
%% SSM END

%%

%% CREEP BEGIN

%% Create directories and filename.

%%% IMPORTANT! To run this m-file, you must change 'dir' to the directory
%%% where the raw files are located on your computer.

%dir = 'E:\Instron Tests\Stepped Isostress\SSM-2\SSM-2.is_tcyclic_RawData\';
dir = 'C:\Users\Chris\Google Drive\UTEP\MERG\Accelerated Creep\Tensile
Tests\3. Creep\CP-2.is_tcyclic_RawData\';
raw = 'Specimen_RawData_1.csv'; % Raw filename for all tests.

file = [dir raw];

%% Import Files

fid = fopen(file);
headers = textscan(fid,'%s',7,'delimiter',','); % There are seven data
columns.
data =
textscan(fid,(repmat('%f',[1,7])),'delimiter',',"','CollectOutput',1,'headerl
ines',2,'MultipleDelimsAsOne',true);
fclose(fid);

temp = cell(1,7);
for i = 1:7
   temp{i} = data{1}(:,i);
end
creepraw = cell2mat(temp);
%%


%% Raw data columns are:
```

```
% |     1    |      2         |     3    |          4           |         5
|          6             |       7         |
% | Time (s) | Extension (in) | Load (N) | Tensile Stress (MPa) | Tensil
Extension (in) | Tensile Strain (in/in) | Epsilon (in/in) |

%% Define variables and constants.

cptime = data{1}(:,1)/3600; % Time in hours
cpepsilon = data{1}(:,7);
cpstress = data{1}(:,4);

ref = [245.72, 249.68, 253.65, 257.61]; % Reference stresses.

%% Initial horizontal offset
% Custom function 'tnot' finds first appreciable value of reference stress
% and deletes all values before it for time, stress, and strain.

C = tnot(cptime,cpstress,cpepsilon,245.7);

% Copy modified time, stress, and strain.
CPTT = C{1};
cpss = C{2};
cpee = C{3};

% Fine tune the modification, the index is including some non-creep strain.
CPTT(1:79) = [];
cpss(1:79) = [];
cpee(1:79) = [];

% Clip the ramp down. NOTE: index is chosen after the time shift.
CPTT(719920:end) = [];
cpss(719920:end) = [];
cpee(719920:end) = [];

%% Adjustment #1 - Vertical Adjustment
    % Make both experiments start at the same value of strain.
    % First value of SSM-2 is 0.02033 (if unmodified).
    % First value of CP-2 is ee(1)

% Find strain difference between CP and SSM at t = 0.
% cpnot = cpee(1); % First strain value of CP-2.
% ssmnot = 0.02033; % First strain value of SSM-2.
% delta = cpnot - ssmnot;
% cpee = cpee - delta; % Shift CP-2 so it starts at the same point as SSM-2.

cpee = cpee - cpee(1); % Vertical shift to zero strain, which is same
starting point as SSM-2.

ssmtt = tcell{1} - tcell{1}(1); % Shift SSM-2 to t = 0.
```

```
ssmee = rcell{1}; % Rename because it's easier to type.

%% Creep Compliance at ref. stress
% CP-2 and SSM-2 (ref. stress)

SSME = cell(1,4); % strain
SSMJ = cell(1,4); % compliance
SSMT = cell(1,4); % time (linearly rescaled)
SSMT0 = cell(1,4); % time (all stresses time-shifted to zero)
for i = 1:4
    SSME{i} = rcell{i}; % Vertically shifted strain, starts at zero.
    SSMT{i} = tsim{1,i}; % Rescaled time: 1 = linear fit, i = stress level.
    SSMJ{i} = SSME{i}/ref(i); % Creep compliance, all SSM-2 stress levels.
    SSMT0{i} = tcell{i} - tcell{i}(1); % Time shifted so all start at zero.
end

ssmjj = ssmee/ref(1); % Creep Compliance, first region of SSM-2.
CPJJ = cpee/ref(1); % Creep compliance, CP-2.

%% Compliance relationships
% CP-2, (slope / ref. slope) & (y-int / ref. y-int)
% Trying to find relationship between creep compliance curves.

jpoly = cell(4,1);
jratio = zeros(4,2);
jyint = zeros(4,1); dint = zeros(4,1);
for i = 1:4
    jpoly{i} = polyfit(SSMT{i},SSMJ{i},1); % polynomial coefficients
    jratio(i,1) = jpoly{i}(1,1)/jpoly{1}(1,1); % (slope / (ref slope))
    jratio(i,2) = jpoly{i}(1,2)/jpoly{1}(1,2); % (y-int/ (ref y-int))
    jyint(i)= jpoly{i}(1,2); % vector just for y-intercepts
        dint(i) = jyint(i)-jyint(1); % difference from ref. y-intercept
end

% Prony Series
% J = J0 + sum(Ji*(exp(-t/tau_i)))

%% Plots %%
%%%%%%%%%%
%%%%%%%%%%
%% Raw data
% CP-2, stress & strain vs. time

% figure
% [ax,h1,h2] = plotyy(time,epsilon,time,stress);
% title('SSM-2 Strain & Stress vs. Time')
% axes(ax(1)); % Set current axes corresposding to 'epsilon'
% xlabel('Time (hours)'), ylabel('Strain (in/in)')
% set(gca,'Xtick', 0:25,'Ytick',0:0.005:0.05), ylim([0 0.05])
```

```
% grid on
% axes(ax(2));
% ylabel('Stress MPa');
% set(gca,'Ytick',0:300/10:300), ylim([0 300])
%
%% Initial Comparison
% CP-2 and SSM-2 (ref. stress)
%
% figure
% plot(ssmtt,ssmee,'.',cptt,cpee,'.')
% title('CP-2 and SSM-2 at ref. stress')
% xlabel('Time (hours)'), ylabel('Strain (in/in)')
% legend('CP-2 (245.72 MPa)','SSM-2 (245.72 MPa)')

%% Creep, no scaling
% SSM-2

figure
for i = 1:4
plot(tcell{i},rcell{i})
    hold on
end
    hold off
title('Creep Strain vs. Time, SSM-2 (no scaling)');
xlabel('Time (Hours)'); ylabel('Creep Strain (in/in)')
legend('245.7 MPa','249.68 MPa','253.65 MPa','257.61
MPa','location','southeast')
%
%% Creep compliance, linear rescale and horizontal shift comparison
% CP-2 (ref.) and SSM-2 (all stress levels)
% Linear plot

phi = [1.6, 1.4, 0.6, 0.4]; % Shift factor, guess

figure
subplot(2,2,1)
for i = 1:4
    plot(SSMT{i},SSMJ{i})
    hold on
end
    plot(CPTT,CPJJ)
    hold off
title('Creep')
xlabel('Time (hours)'), ylabel('Strain (in/in)')

subplot(2,2,2)
%%
for i = 1:4
    plot(SSMT{i}./phi(i),SSMJ{i})
```

```
    hold on
end
    plot(CPTT,CPJJ)
    hold off
title('Creep, horizontally shifted')
xlabel('Time (hours)'), ylabel('Strain (in/in)')
%%
% Creep compliance, linear rescale and horizontal shift comparison
% CP-2 (ref.) and SSM-2 (all stress levels)
% Semilog plot
subplot(2,2,3)
for i = 1:4
semilogx(SSMT{i},SSMJ{i})
    hold on
end
semilogx(CPTT,CPJJ)
    hold off
title('Creep Compliance')
xlabel('Time (log(hours))'), ylabel('Creep Compliance (MPa^{-1})')

subplot(2,2,4)
for i = 1:4
semilogx(SSMT{i}./phi(i),SSMJ{i})
    hold on
end
semilogx(CPTT,CPJJ)
    hold off
title('Creep Compliance, horizontally shifted')
xlabel('Time (log(hours))'), ylabel('Creep Compliance (MPa^{-1})')
legend('SSM-2 (245.72 MPa)','SSM-2 (249.68 MPa)','SSM-2 (253.65 MPa)','SSM-2
(257.61 MPa)','CP-2 (245.72
MPa)','Location','southeast','orientation','horizontal')


%% Creep Compliance at ref. stress
% CP-2 and SSM-2 (ref. stress)

figure
   plot(SSMT{1},SSMJ{1})
   hold on
   plot(CPTT,CPJJ)
   hold off
title('Creep Complianceof CP-2 and SSM-2 at ref. stress')
xlabel('Time (log(hours))'), ylabel('Creep Compliance (MPa^{-1}')
legend('CP-2 (245.72 MPa)','SSM-2 (245.72 MPa)')
%
%% Creep Compliance, shifted to zero
% SSM-2
%
```

```
% t0shift = [0.8, 0.6, 0.4, 0.2];
%
% figure
% subplot(1,2,1)
% for i = 1:4
%    plot(SSMT{i}/t0shift(i),SSMJ{i})
%    hold on
% end
%    hold off
% title('Creep Compliance Shifted to Zero, SSM-2')
% xlabel('Time (hours)'), ylabel('Creep Compliance (MPa^{-1})')
% legend('245.7 MPa','249.68 MPa','253.65 MPa','257.61
MPa','location','southeast')
%
% subplot(1,2,2)
% for i = 1:4
%    semilogx(SSMT{i}/t0shift(i),SSMJ{i})
%    hold on
% end
%    hold off
% title('Creep Compliance Shifted to Zero, SSM-2')
% xlabel('Time (hours)'), ylabel('Creep Compliance (MPa^{-1})')
% legend('245.7 MPa','249.68 MPa','253.65 MPa','257.61
MPa','location','southeast')

%% Creep Compliance, shift factor
% CP-2

shift = [0.8, 0.6, 0.4, 0.2];
hshift = [0 5 10 15];
figure
for i = 1:4
   plot(SSMT0{i}./shift(i),SSMJ{i})
   hold on
end
plot(CPTT,CPJJ)
hold off
title('Creep Compliance SSM-2, shift factor applied')
xlabel('Time (hours)'), ylabel('Creep Compliance (MPa^{-1})')
legend('245.7 MPa','249.68 MPa','253.65 MPa','257.61 MPa','CP-2','SSM-
2','location','southeast')

%% Creep Compliance, forced superposition
% CP-2

figure
for i = 1:4
   plot(SSMT0{i},SSMJ{i}-dint(i)) % force all curves to superimpose, based on
their y-intercepts
```

```
   hold on
end
hold off
title('Creep Compliance, Shifted SSM-2')
xlabel('Time (hours)'), ylabel('Creep Compliance (MPa^{-1})')
legend('245.7 MPa','249.68 MPa','253.65 MPa','257.61
MPa','location','southeast')
%% Compliance relationships
% CP-2, (slope / ref. slope) & (y-int / ref. y-int)
%
% figure
% plot(1:4,jratio(1:4),'.',1:4,jratio(5:8),'.','MarkerSize',32)
% title('Creep compliance relationships')
% legend('slope/ref','y-int/ref','Location','Southeast')
% set(gca,'Xtick',1:4)
% grid on

%% What is this?
% tshift = cell(1,length(tcell{1}));
% for i = 1:length(ssmtt)
% tshift{i} = ssmtt - sstt(1);
% end

%% CREEP END
```

Vita

Christopher Ramirez began his academic journey in 2009, when he decided to pursue physics in the hopes of studying the cosmos. He performed research in the UTEP Physics Department calculating the energy of diatomic molecules, while tutoring undergraduate students in physics and mathematics. His research caught the attention of Kansas State University, where he participated in a Research Experience for Undergraduates in plasmonics and optics. He then went on to attend two back-to-back internships at NASA's Glenn Research Center, where he studied the mechanical properties of carbon nanotubes and the heat transfer properties of silica aerogels.

His work at NASA helped guide his aspirations to mechanical engineering, and he soon applied to UTEP's Master's of Science in Mechanical Engineering graduate program. He began his work for Calvin M. Stewart, under the Materials at Extremes Research Group. Here, he enabled the research group to perform three-dimensional digital image correlation experiments and developed an accelerated creep testing method. His work in assessing a large database of creep rupture data is currently being reviewed by the International Pressure Vessel and Piping Journal.

Contact Information: ramirez.christopher@gmail.com

This thesis/dissertation was typed by Christopher Ramirez.